Spring 4-22-2020

Optimization of ADC linkers: design and evaluation of a FRET-based ADC linker-library

Jared T. Miller

OPTIMIZATION OF ADC LINKERS: DESIGN AND EVALUATION OF A FRET-BASED ADC LINKER-LIBRARY

BY

JARED T. MILLER

THESIS

Submitted in partial fulfillment of the requirement for
Honors Thesis in Biochemistry
in Harpur College of Arts and Sciences of
Binghamton University
State University of New York
2020

Accepted in partial fulfillment of the requirement for
Honors Thesis in Biochemistry
in Harpur College of Arts and Sciences of
Binghamton University
State University of New York
2020

April 20, 2020

Dr. L. Nathan Tumey, Faculty Advisor
Department of Pharmacy and Pharmaceutical Sciences, Binghamton University

Dr. Susan C. Flynn, Member
Department of Chemistry, Binghamton University

Dr. Ming An, Member
Department of Chemistry, Binghamton University

Abstract

Success of Antibody-drug conjugates (ADCs) relies on the maintained integrity of a chemical linker fusing a therapeutic payload to a monoclonal antibody. Recent reports have revealed the lead linker ValCitPABC has poor stability in rodent models compared to mammalian counterparts, resulting in many clinical investigations predicting poorer ADC efficacy due to premature payload release in these model systems. Optimization of this chemical linker to be resistant both in mouse and human models would streamline ADC progression into clinical trials. Herein we describe the synthesis and development of a FRET-based assay for evaluating linker stability *in vitro*. Evaluation of lysosomal release by catabolic proteases paired with serum stability testing identified a series of asparagine containing linkers which surpassed both the release kinetics and stability profiles of ValCitPABC. A synthetic scheme for MMAE attachment to these asparagine linkers was established. Ultimately, this work lays a foundation for future evaluation of these linker *in vivo* for the identification of next generation peptide linkers to surpass the limitations of ValCitPABC.

Table of Contents

List of Tables

Tables

HPLC/UPLC Solvent Gradient Tables

Supplemental Material

List of Figures

Figures

Synthetic Schemes

Supplemental

List of Abbreviations

General Biology
ADC – Antibody-Drug Conjugate
mAb – Monoclonal Antibody
Ces1C – Carboxyesterase 1C

Cytotoxic Payloads
PBD – Pyrrolobenzodiazepine
DUO – Duocarmycin
MMAE – Monomethyl Auristatin E
MMAF – Monomethyl Auristatin F
DM1 – Mertansine

Linkers Component Chemistry
mcValCitPABC – Maleimide Caproyl Valine Citrulline p-Aminobenzyl Carbamate
Mal - Maleimide
AEEA – Amino Ethoxy Ethoxy Acetic Acid
PABC – p-Aminobenzyl Carbamate
PABA – p-Aminobenzyl Amide
PAB-OH – p-aminobenzyl alcohol
PNP – p-Nitrophenol
FRET – Forester Resonance Energy Transfer
TAMRA – Tetramethylrhodamine
OG – Oregon Green (Fluorescein)

Organic Reagents
DIPEA – Diisopropylethylamine
HATU – Hexafluorophosphate Azabenzotriazole Tetramethyl Uronium
EDC – 1-Ethyl-3-(3-dimethylaminopropyl) carbodiimide
HOBt – Hydroxybenzotriazole
HOAt – 1-Hydroxy-7-azabenzotriazole
TFA – Trifluoroacetic Acid
DTT – Dithiothreitol

Organic Solvents
DMA – Dimethylacetamide
DMF – Dimethylforamide
DCM – Dichloromethane
ACN – Acetonitrile

Amino Acid Abbreviations
1Nal – 1-napthalene
2Nal – 2-napthalene
Aib – α-Aminoisobutyric Acid
Ala – Alanine
Asn – Asparagine
Cit – Citrulline
Cys – Cysteine
Gln – Glutamine
Gly – Glycine
His – Histidine
Ile – Isoleucine
Lys – Lysine
Phe - Phenylalanine
Pro – Proline
Ser – Serine
Trp – Tryptophan
Tyr – Tyrosine
Val – Valine

1 Introduction

1.1 Antibody Drug Conjugate Composition

Targeted-drug delivery has grown in prevalence over the past several decades as a means to bypass off target side effects from systemic administration of a biologically active compound.[1] This philosophy has grown in importance within oncology, where classical cytotoxic agents have targeted rapidly dividing malignant cells, concurrently acting on erythrocytes, leukocytes, and keratinocytes leading to problematic side effects. Antibody-drug conjugates (ADC) offer an active targeting mechanism to eliminate a cell type of interest by fusing a potent payload to an antibody which recognizes a selectively expressed cell surface antigen.[2] Comprised of a monoclonal antibody, chemical linker and therapeutic payload, ADC efficacy and pharmacokinetics are entangled with the interactions between these three components and the cell machinery they come in contact with.

Careful payload delivery is achieved through the selection of a monoclonal antibody (mAb) with high affinity towards a selectively expressed cell surface antigen. The targeted receptor must maintain a mechanism of clathrin-mediated endocytosis to enable ADC entry into the cell for internal payload release.[2] Most ADC applications see light in oncology, with typical cytotoxic payloads interacting with DNA (PBD, DUO) or microtubules (MMAE, MMAF, DM1).[3–7] Ideally, a payload should be released from the conjugate in an unmodified state, but several payloads have been demonstrated to tolerate structural modifications at the linkage site.[6,8] The linker chemistry conjoins the payload to a mAb and contains a controlled mechanism of release spanning disulfide, hydrazone, and peptide functionalities which exploit the intracellular environment (glutathione reduction of disulfides in cytoplasm, acid hydrolysis of hydrazones in lysosome, and proteolytic cleavage of peptide linkers).[9,10] Fusion of the linker-payload to the antibody is accomplished through conjugation strategies including lysine amide coupling, cysteine coupling and enzymatic conjugation.[10] Given the four native cysteine disulfide linkages in mAbs, cysteine conjugation is a simple and reliable method of attaching upwards of eight payloads to a single ADC. Successful advancements in ADC development has revolved around the

optimization of this linkage, as pharmacokinetic parameters of stability in circulation, rate of release and catabolic transformation encompass linker chemistries. Currently, five ADCs are approved for clinical use by the US Food and Drug Administration (FDA) with over 80 currently in clinical trials, demonstrating the exciting promise this modality brings to therapeutic applications.[9]

1.2 The mcValCitPABC Lead Linker and Extracellular Stability Concerns

Currently, two FDA approved ADCs, Adcetris and Polivy, utilize a cysteine conjugation technique and proteolytic release mechanism with a leading Valine-Citrulline-p-aminobenzyl carbamate (ValCitPABC) linker.[11,12] Payload release from ValCitPABC utilizes cathepsin B, a cysteine protease, to hydrolyze the amide bond between citrulline and PABC, forcing 1,4-elimination mechanism to release the unmodified payload (fig. 1). Like all linkers, this cleavage mechanism is essential for successful payload release internally but comes with the caveat of resisting enzymatic cleavage while in circulation.

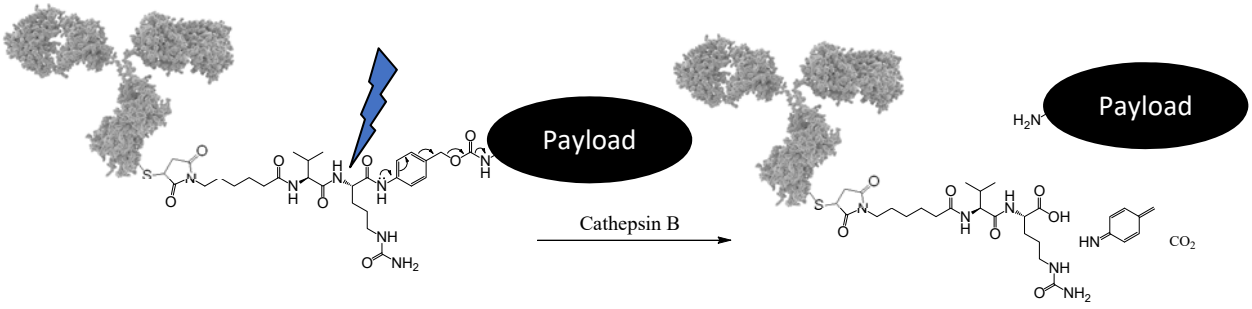

Figure 1. Cathepsin B Mediated cleavage and subsequent 1,4-elimination of the payload

Recent discoveries have revealed the ValCitPABC linker to be more unstable in circulation than previously believed. Surprisingly, an extracellular serine hydrolase Carboxyesterase 1C (Ces1C) was identified as capable of releasing payloads.[13] While believed to hydrolyze the amide bond adjacent to PABC like lysosomal proteases, additional reports indicate the carbamate may susceptible to hydrolysis by Ces1C resulting in payload loss as well.[14] These stability concerns are most prevalent in mouse and rat studies, with primate studies revealing less significant cleavage.[15] This stability differential is problematic for evaluating potential ADC efficacy and safety, as non-primate models are used as a primary method of triaging drug candidates. Utilization of Ces1C knockout mice can mitigate this concern but demand a long

lead time for *in vivo* studies.[14] While site-selective ADCs showed promise in enhancing stability, recent reports these selections also result in premature payload release.[16] In addition to Ces1C, neutrophil elastase has been shown to hydrolyze the ValCitPABC linker resulting in neutropenia.[17]

The most promising method to alleviate these concerns have involved modifications to the amino acid composition at the P_3 position of P_3-Val-Cit-PABC linkages, resulting in more robust linkers in mouse models.[13,18] We have adopted a similar methodology, by interrogating both the P_2 and P_1 positions of the linker in hopes of identifying a series of linker chemistries with enhanced extracellular stability profiles while still utilizing a proteolytic lysosomal release mechanism.

2 Methodology

2.1 Linker Design

Linkers were designed to mimic the structure of mcValCitPABC while retaining a synthesis to allow an easy interchange of amino acids to interrogate the P_1 and P_2 positions of proteases. The resulting Mal-AEEA-Gly-P_2-P_1-COOH linker was designed as a model system matching the above criterion. An N-terminal maleimide enabled future Michael addition including cysteine conjugations, the AEEA-Gly components mimicked the caproyl spacer seen in the traditional linker, and the P_2 and P_1 positions held varying amino acids chosen to span chemical space. A total of 75 peptides were prepared by WuXi AppTec providing 15-30mg of each designed peptide. Completing the mimic of mcValCitPABC, a p-aminobenzyl amine moiety was attached to the C-terminus of Mal-AEEA-Gly-P_2-P_1-COOH linkers, and an amide linkage at the benzylic position connected a desired payload for screening purposes (Fig. 2A).

2.2 FRET-Based Assay

Screening of lysosomal lability and extracellular stability of each proposed linker was achieved through a FRET based assay. An Oregon Green fluorophore (ex. 488nm, em. 520nm) was coupled to the C-terminal benzylic amine forming the donor, while an N-terminal TAMRA fluorophore (ex. 550, em. 575) was linked through Michael addition at the maleimide to form the acceptor chromophore of the FRET pair.

While the linker within the FRET pair is stable, Oregon Green fluorescence signaling is absent (Fig. 2B-C). When cleaved, an increase in Oregon Green fluorescence can be monitored over time, which can be correlated with a stoichiometric equivalence of payload release, allowing a quantitative measurement of linker cleavage over time.

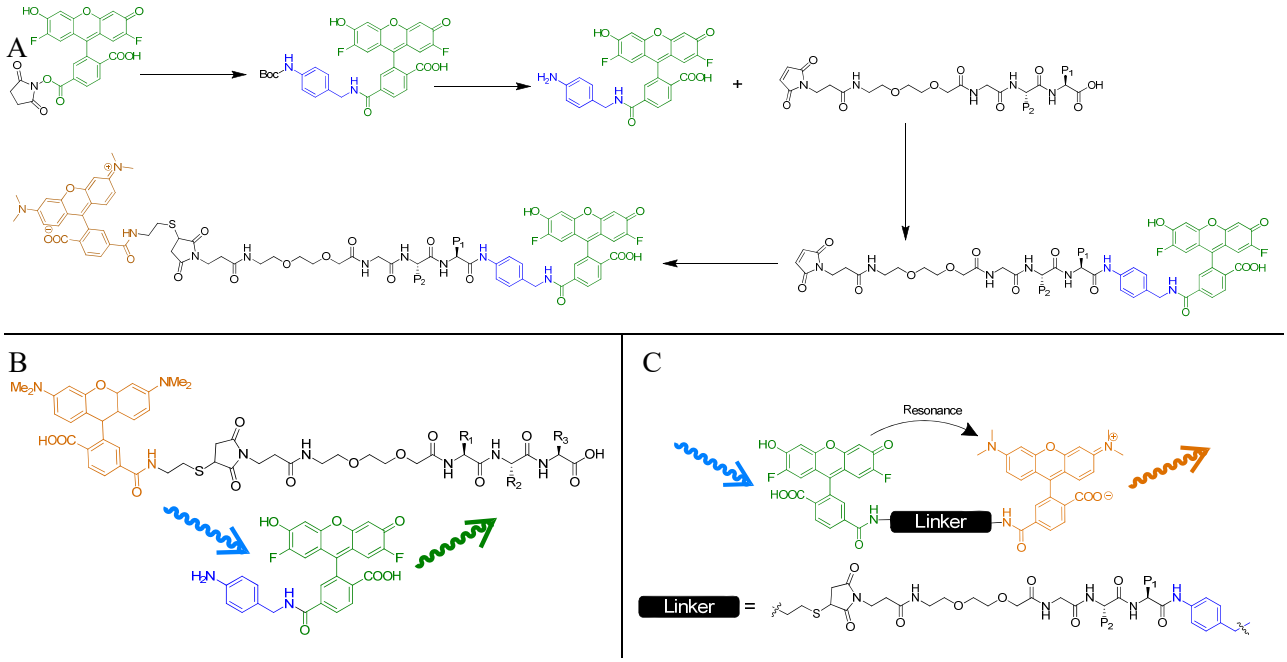

Figure 2. Synthetic proposal and chemical basis of a FRET-based assay. A) Synthesis of FRET Pairs. Oregon Green is indicated in green, PABC aryl mimic in blue, and TAMRA in orange. B) Cleavage of FRET Pair results in Oregon Green release, allowing Oregon Green fluorescence. C) Resistance to cleavage maintains the FRET pair, retaining resonance to prevent Oregon green fluorescence.

2.3 Statement of Purpose

The goal of this work is to screen a library of peptide linkers using a FRET-based assay to identify linkers that surpass stability profile of mcValCitPABC. Screening this library against lysosomal enzymes validates a linker's potential to release a payload effectively intracellularly, while screening against known extracellular hydrolases identifies linkers with higher resistance to premature payload release. Additionally, monitoring release in serum provides a holistic picture of extracellular stability as opposed to individual evaluation of a single enzyme. Herein, we report the synthesis of this FRET library, evaluation of linkers against intra and extracellular conditions, identification of linkers with interesting stability profiles and synthesis of linker payloads using identified peptides is described.

3 Results and Discussion

3.1 Synthesis of FRET Library

Synthesis of FRET pairs began with the addition of Boc-p-aminobenzyl amine to Oregon Green NHS ester **(1)**, and subsequent deprotection to yield the aniline **(3)**. Coupling the aniline **(3)** to the C-terminus of peptides **(4)** was dependent on the coupling reagents used. Generally, HATU coupling was sufficient for amide bond formation, but was found to acylate histidine, forming a 1,1,3,3-tetramethylguanidine group on the ε-amine. This undesirable side-product was eliminated by substituting the coupling reagent to EDC. In reactions wherein the peptide contained a lysine, the aniline was used in threefold excess in order to outcompete intramolecular cyclization. For all conditions, fifteen reactions were performed in parallel in 2-dram vials and purified by an automated mass-directed LC/MS. Lastly, Michael addition of TAMRA-thiol to the N-terminal maleimide **(5)** under basic conditions completed the formation of the FRET pair **(6)** (scheme 1). Following this route, a total of 75 FRET pairs were synthesized for evaluation. Quenching of Oregon Green fluorescence (typically 50%-80% of the original sample) was observed upon addition of the thiol, thus indicating both the success of the Michael addition and energy transfer within the FRET pair (Table S1).

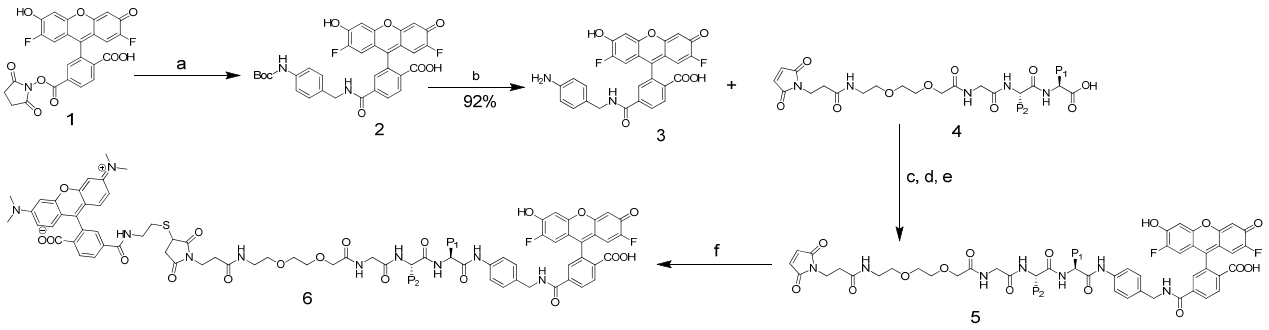

Scheme 1. Synthetic scheme of FRET Pairs. (a) Boc-p-aminobenzylamine, DIPEA, DMF, rt. 4 hr. (b) TFA, DCM, rt. 1 hr. (c) General Conditions: HATU, HOBt, 2,6-Lutidine, rt. 16 hr. (d) P1, P2 = His: EDC, HOBt, 2,6-Lutidine, rt. 16 hr. (e) P2 = Lys: 3 (3 eq.), HATU, HOBt, 2,6-Lutidine, rt. 16 hr. (f) 10% Tris pH 8.0 in DMA, rt. 30 min.

3.2 Lysosomal Lability Screening and SAR Relationships of Catabolic Enzymes

Screening of this synthesized FRET library began with cathepsin B, a known catabolic enzyme of ValCitPABC (Fig. 3A).[19] Cathepsin B was found to cleave the control ValCit linker with the fastest velocity with a large differential between the negative control D-ValD-Cit (Fig. 3B). Most peptides falling within this range shared a similar motif within the P_2 and P_1 positions, with large, hydrophobic amino acids occupying the P_2 positions (Tyr, Ile). Long aliphatic chains with a hydrogen bond donor (Cit, Lys) or small hydrophobic residues (Ala) were permitted in the P_2 site. Substrate specificity is comparable to previously reported findings on the selectivity filters of cathepsin B.[20]

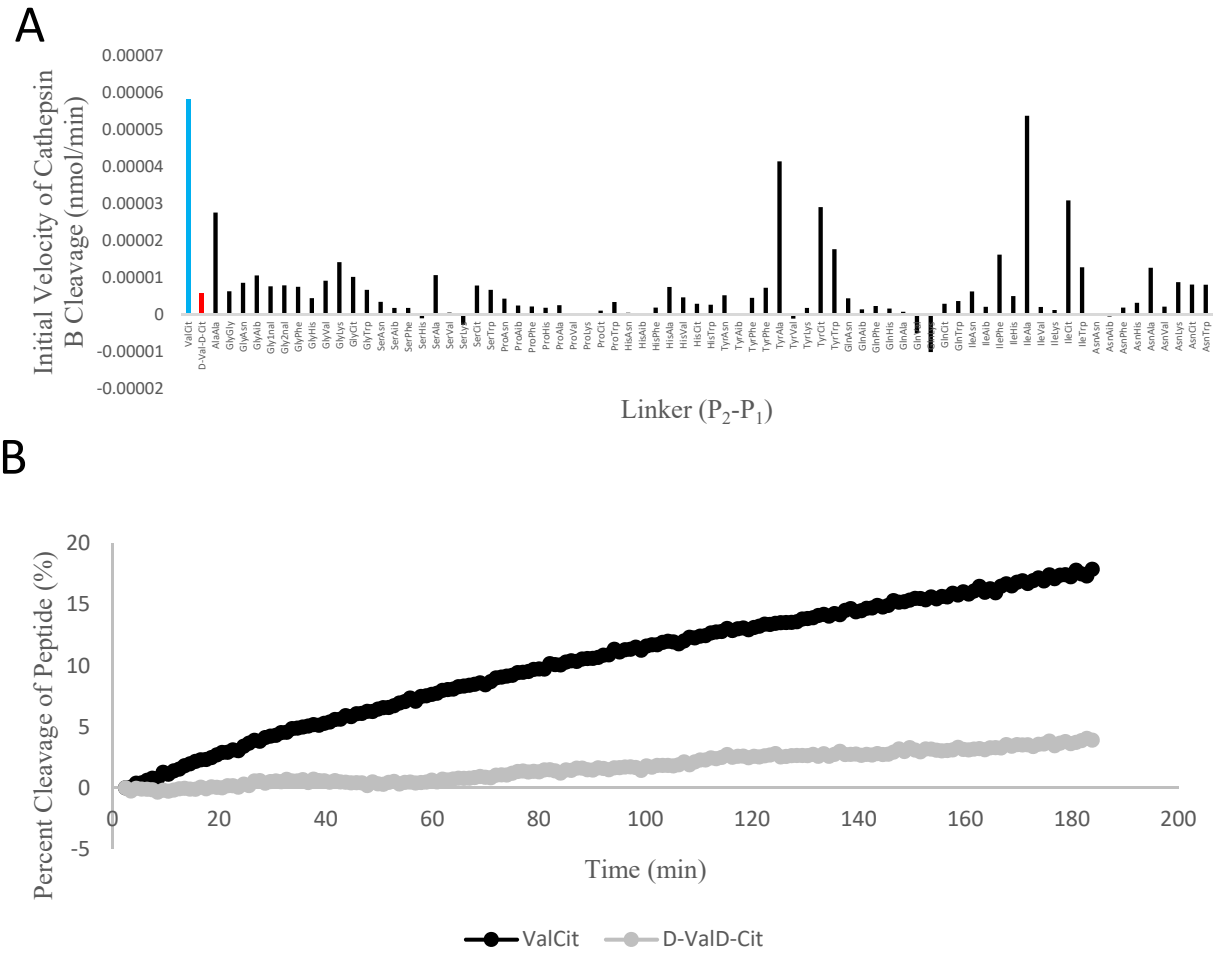

Figure 3. Cathepsin B Catabolism Studies. ValCit positive control is indicated in blue, and D-ValD-Cit negative control is indicated in red. A. Cathepsin B hydrolysis during 12-hour incubation of FRET pairs at 2µg/ml enzyme concentration. B Kinetic plot of positive (ValCit) and negative controls (D-ValD-Cit) to show cleavage differential.

Next we turned to using rat liver trisotomes, lysosomal prep taken from rats, containing a multitude of lysosomal enzymes including the previously evaluated cathepsin B. Exposure of the FRET pairs to rat liver tritosomes provided a broader, holistic picture of lysosomal cleavage compared to single enzyme evaluations (Fig. 4A). As expected, the peptides rapidly cleaved by cathepsin B (Fig. 3A) were shown to be cleaved at comparable rates by the tritosomes (Fig. 4A). Unlike the results from the cathepsin B study, many linkers exhibited faster rates of cleavage compared to than the ValCit Comparator (Fig. 4A). Interestingly, many of the rapidly cleaved linkers shared the structural motif of an asparagine occupying the P_2 or P_1 positions. Furthermore, these linkers were demonstrated the be poorly hydrolyzed by cathepsin B, strongly suggesting the presence of a unique protease as a potential vector for enzyme-mediated drug release. The conserved nature of asparagine residues within the linker pointed to legumain, an asparagine endopeptidase, as the source of this observation.[21]

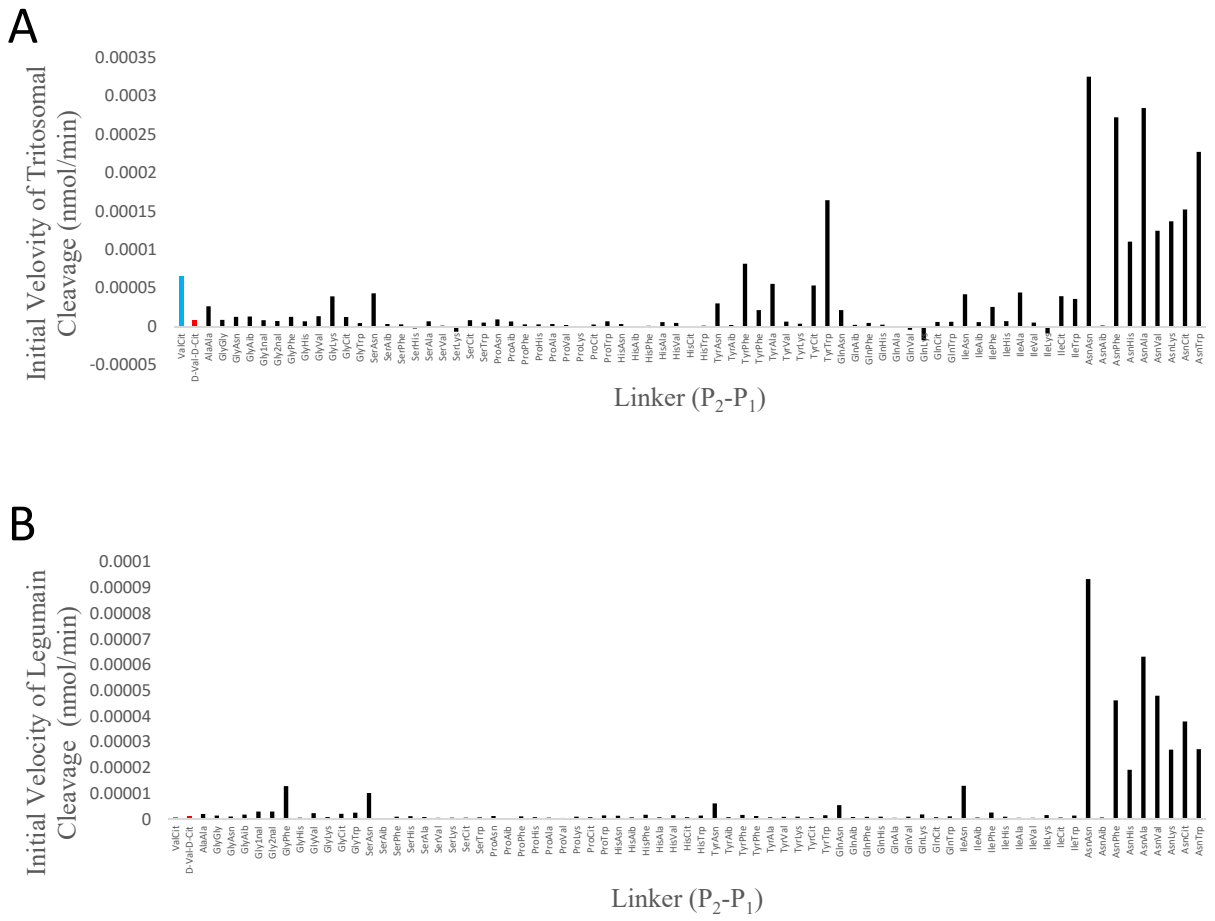

Figure 4. Rat Liver Tritosomes and Legumain Catabolism Studies. ValCit positive control is indicated in blue, and D-ValD-Cit negative control is indicated in red. A. Tritosomal hydrolysis during 6.5-hour incubation of FRET pairs at 37.5 µg/ml enzyme concentration. B. Legumain hydrolysis during 12-hour incubation of FRET pairs at 5.0 µg/ml enzyme concentration.

Evaluation of legumain cleavage of this FRET library revealed identical trends between asparagine containing linkers and rates of hydrolysis, with P_2 asparagine linkers being hydrolyzed more readily than P_1 asparagine linkers (Fig. 4B). Legumain also was demonstrated to be highly specific for asparagine containing linkers, in line with its known catabolic role.[21] Interestingly, selectivity filters of legumain have been shown to allow asparagine occupation of the S_1 site with a versatile S_1' site, enabling legumain to generate C-terminal asparagine peptide fragments exclusively.[21] This indicates hydrolysis of peptides with asparagine in the P_2 position results in the release of an undesirable amino acid linked payload (Fig. 5A). The slower velocity of legumain on P_1 asparagine containing linkers indicates the desired cleavage

before the aniline is possible, but the occupation of the aryl group within the S_1' site may disfavor binding to legumain. The removal of the self-immolative PABC spacer would be synthetically efficient for linker payload synthesis and may allow release of the unmodified payload at more rapid kinetic rates (Fig. 5B). Additionally, the hydrolysis of AsnVal gives hope for the release of MMAE using a terminal Asn linker, as MMAE contains an N-methylated valine residue within its structure which would be attached to a linker's C-terminus. Like cathepsin B, legumain has been shown to be upregulated in the tumor microenvironment, enhancing its potential as a vector for ADC payload release in oncological applications.[8]

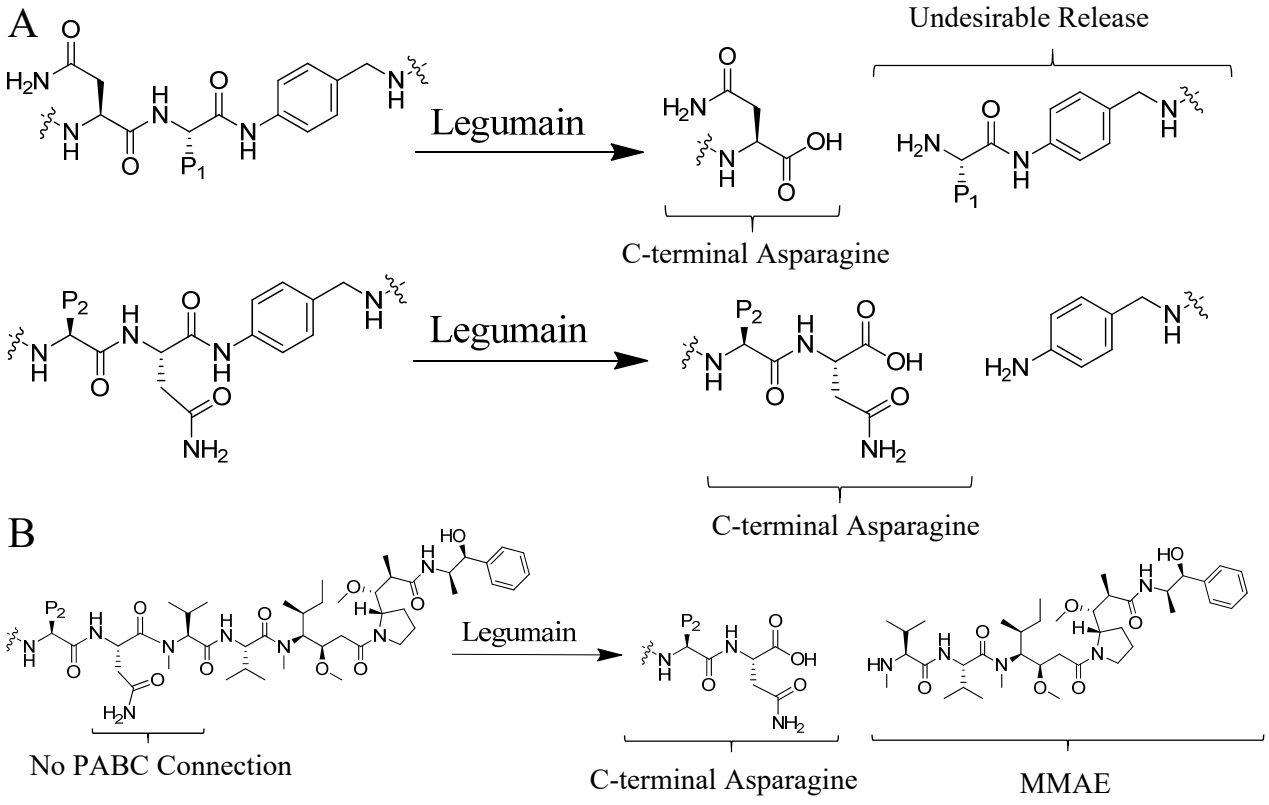

Figure 5. Illustration of Legumain Cleavage. A) Legumain cleaves resulting in C-terminal asparagine peptide fragments. B) Attachment of MMAE to the C-terminus of the linker may allow for direct payload release.

3.3 Extracellular Stability Screening and SAR Relationship of Ces1C

Resistance of linkers to promiscuous extracellular hydrolase Ces1C was performed and revealed interesting structural motifs (Fig. 6A). Hydrolysis of tryptophan containing linkers was most rapid, with all linkers showing varying degrees of susceptibility. Unexpectedly, P_2 citrulline and valine containing linkers were the most resistant to cleavage by Ces1C, with the lead linker ValCit showing the most impressive resistance. This was surprising considering that multiple papers have demonstrated that ValCit-PABC linkers are cleaved by Ces1C.[13–16] However, conflicting reports in the literature indicate Ces1C cleaves at the C-terminus of the linker, while others report a hydrolysis of the carbamate resulting in acylation of the Ces1C catalytic serine.[13,14] The lack of a carbamate linkage in our model system may rationalize some resistance our library has to Ces1C. The proposed removal PABC through legumain-mediated release may circumvent this potential of Ces1C hydrolysis at the carbamate linkage. Additionally, most attempts to mitigate Ces1C activity on linkers target the P_3 position adding unique functionalities, where our library contains an unhindered glycine in that position that would not prevent Ces1C activity.[13,18] Amino acid extension at the C-terminus would allow for an expansive library, shifting the current P_2 amino acid to the P_3 position, allowing us to monitor the impact this site has on linker catabolism.

Stability of linkers within mouse and human serum varied, with more linkers showing instability within mouse serum (Fig. 6B, C). ValCit was shown to release 5% and 10% payload over 18 hours in mouse and human serum respectively. Tryptophan containing linkers were most readily cleaved in mouse serum, likely due to the presence of mouse Ces1C as shown previously. Furthermore, proline and tyrosine in the P_2 position of linkers showed greater payload release over time. The degree of payload release within human serums was much lower but shared the same structural motifs of proline and tyrosine linker hydrolysis. In addition, we observed that P_2 histidine-containing linkers exhibited relatively high degrees of cleavage. Importantly, most asparagine containing linkers, with asparagine occupying both the P_1 and P_2 positions, were shown to be highly resistant to hydrolysis in mouse and human serum.

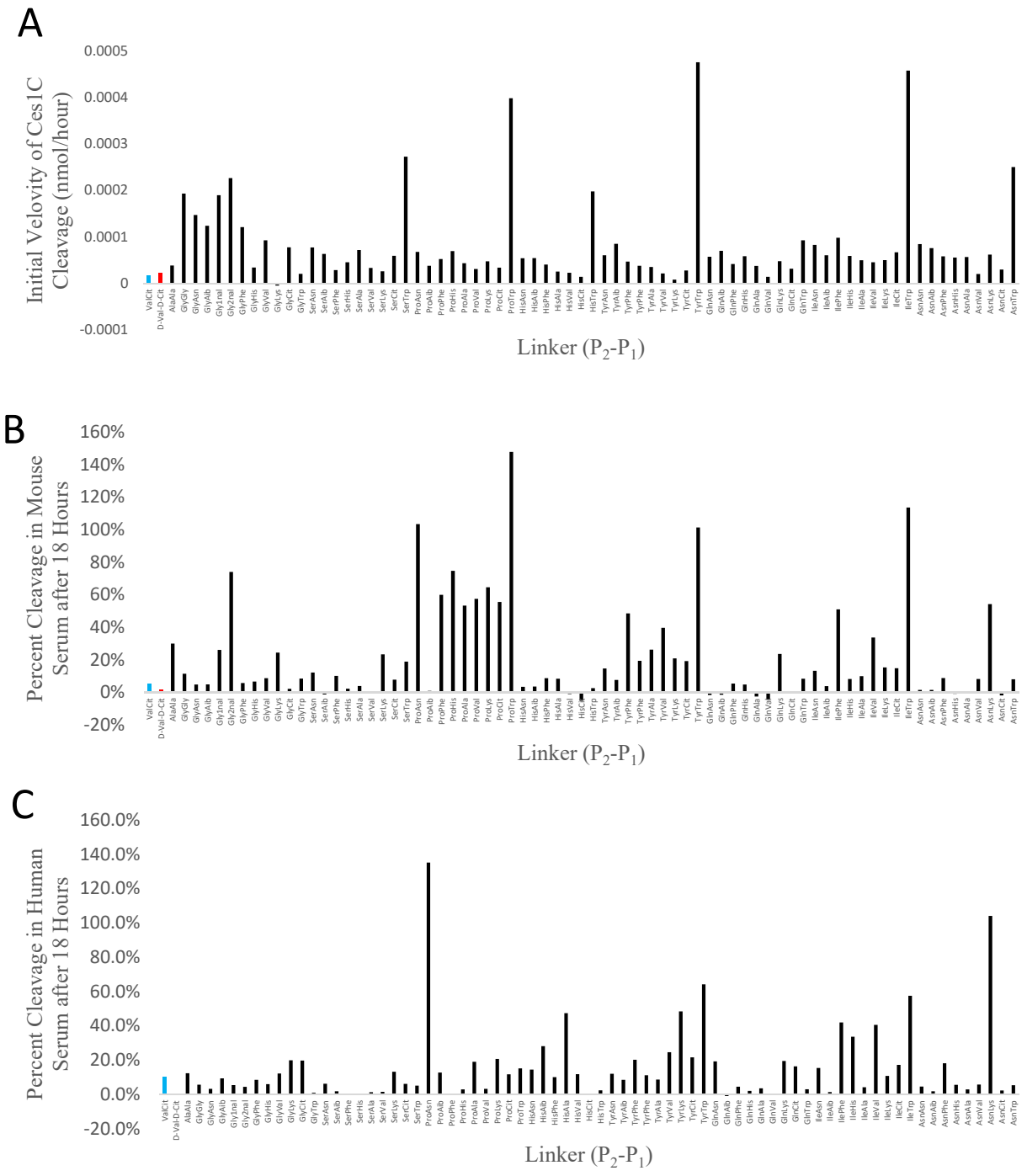

Figure 6. Stability evaluation of linkers against Ces1C and serum. ValCit positive control is indicated in blue, and D-ValD-Cit negative control is indicated in red. Ces1C stability is reported in terms of initial velocity of cleavage, and serum stability is reported in terms of percent cleavage. A. Ces1C hydrolysis during 10-day incubation of FRET pairs at 10.0µg/ml enzyme concentration. B. Mouse serum stability over 18 hours. C. Human serum stability over 18 hours.

3.4 Identification of Optimal Linker Chemistries for MMAE Linker Payloads

The rapid hydrolysis of asparagine containing linkers in lysosomes paired with the enhanced stability within serum indicates high potential for ADC applications. Linker payload synthesis of identified linkers was developed using MMAE as the payload of choice, as its cytotoxic activity is nullified if released in its non-native form (Table 1).[22] The hypothesis that legumain may not release the unmodified payload resulted in the subdivision of asparagine linkers into two groups for future evaluation. Serum stable linkers SerAsn, GlnAsn and AsnAsn containing a P_1 asparagine are believed to be cleaved at the P_1 position to liberate an unmodified payload, and therefore are hypothesized to be biologically active using MMAE. In contrast, the linker AsnAla is shown to be lysosomally labile and extracellularly stable but is hypothesized to not be biologically active by releasing a modified, amino acid linked MMAE payload. To evaluate the accuracy of our model system in predicting ADC stability and release, TyrTrp was selected as a readily hydrolyzed linker in both the lysosome and serum. Conversely, GlnVal was selected as a negative control, being resistant to hydrolysis in both the lysosome and serum.

Table 1. Identified Linkers for MMAE Attachment and Reported Stability Profile

Linker-Payload Chemistry	Lysosomal Release (Enzyme)	Serum Stable	Hypothesized Biological Activity
3-Mal-AEEA-Gly-Val-Cit-PABC-MMAE	Yes (Cathepsin B)	Yes	Active (Positive Control)
3-Mal-AEEA-Gly-Ser-Asn-PABC-MMAE	Yes (Legumain)	Yes	Active
3-Mal-AEEA-Gly-Tyr-Trp-PABC-MMAE	Yes (Cathepsin B)	No	Active
3-Mal-AEEA-Gly-Gln-Asn-PABC-MMAE	Yes (Legumain)	Yes	Active
3-Mal-AEEA-Gly-Gln-Val-PABC-MMAE	No	Yes	Inactive (Negative Control)
3-Mal-AEEA-Gly-Asn-Asn-PABC-MMAE	Yes (Legumain)	Yes	Active
3-Mal-AEEA-Gly-Asn-Ala-PABC-MMAE	Yes (Legumain)	Yes	Inactive

3.5 Synthesis of MMAE-Linker Payloads

Identified linkers were taken through a three-step synthesis to attach a PABC spacer and MMAE to each linker (scheme 2). Using HATU coupling conditions known to attach Oregon Green, p-aminobenzyl alcohol was coupled to the C-terminus of each linker **(4)**. The resulting product **(7)** was purified by preparative HPLC. Activation of the benzylic alcohol with bis-p-nitrophenyl carbonate was performed *in*

situ, followed by substitution using MMAE yielded the final linker payload **(9)**. Material was purified by preparative HPLC and characterized by MS and HPLC. Conventional cysteine conjugation to an anti-Her2 antibody will allow these linker payloads to constitute the final ADCs which will be evaluated for cytotoxicity against a breat-cancer cell line at a later date. Attempts to directly attach MMAE to the C-terminus directly were unsuccessful and will be approached in the future as well.

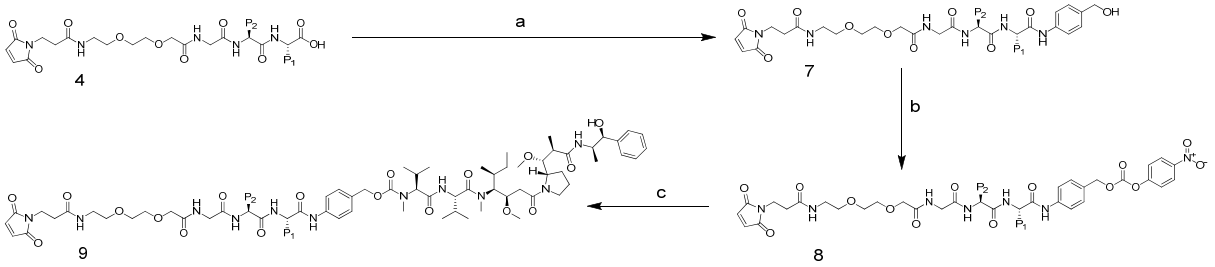

Scheme 2. Synthetic scheme of MMAE Linker Payloads. (a) HATU, HOBt, 2,6-Lutidine, rt. 2 hr. (b) Bis-p-nitrophenyl carbonate, DIPEA, 24 hr. (c) MMAE, HOAt, DIPEA, 2,6-Lutidine, rt. 48 hr.

4 Conclusion

Evaluation of ADC linker stability was successfully performed using a novel FRET-based assay to elucidate the stability profiles of various chemical linkers. Linker lability in the presence of lysosomal proteases identified a series of asparagine containing linkers, which were identified to be hydrolyzed efficiently by the asparagine endopeptidase legumain. The preference of legumain cleavage towards P_2 asparagine linkers alongside the known selectivity of legumain hypothesize that a PABC spacer is poorly tolerated by this peptidase. Given the success of cleaving P_1 asparagine linkers with legumain, it is believed removing the PABC spacer could allow for the direct release of payload alongside being synthetically useful in linker payload synthesis.

Evaluating extracellular stability of these linkers revealed this asparagine series of linkers also retained optimal stability within mouse and human serum. Ces1C screening additionally showed most asparagine-containing linkers to be resistant to this promiscuous hydrolase and identified a structural preference of Ces1C against tryptophan containing linkers. Ultimately, combined screening of lysosomal and

extracellular conditions identified six unique linkers for evaluation in ADC applications. The synthesis of linker payloads was performed allowing future conjugation to monoclonal antibodies for ADC evaluation of cytotoxicity and ADC stability. Additional directions to pursue include the synthesis of C-terminal asparagine coupled MMAE linker payloads for the evaluation of cytotoxicity in the absence of the PABC self-immolative spacer. Ultimately, this work has identified a novel vector for enzyme-mediated payload release for ADC applications alongside the identification of several linkers with enhanced stability profiles that we hope will lead to a new generation of ADC linkers to surpass the limitations of ValCitPABC.

5 Experimental Methods

5.1 Analytical UPLC/HPLC Methods

5.1.1 Normal UPLC-MS Method

Analytical characterization was performed using a Water Acquity H-Class UPLC ® with TUV detector, FLR detector, and QDa mass spectrometer. Typically, 1µl injections were separated using an Acquity UPLC BEH C18 1.7 µm column (2.1 x 50mm) at 80°C. Eluent was monitored by UV (220 and 254nm), fluorescence (ex. 488nm, em. 520nm) and mass spectrometry (150-1250 Da, ES+/ES-). Solvents for the mobile phase were water with 0.1% formic acid (solvent A) and acetonitrile (ACN) with 0.1% formic acid (solvent B). Flow rate was 0.8 ml/min. Gradient Used: Isocratic solvent B for 0.8 min (0-0.8min), then gradient from 10%-95% Solvent B over 4.2 min (0.8-4.5min), isocratic solvent B for 0.3 min (4.5-4.8min), then gradient from 95% solvent B over 0.1 min (4.8-4.9min), then isocratic solvent B for 0.1 min (4.9-5.0min) (Table I).

Table I. Solvent Gradient of Normal UPLC-MS Method

Time (min)	Flow Rate (ml/min)	%A	%B
Initial	0.80	90.0%	10.0%
0.80	0.80	90.0%	10.0%
4.50	0.80	10.0%	90.0%
4.80	0.80	10.0%	90.0%
4.90	0.80	90.0%	10.0%

5.00	0.80	90.0%	10.0%

5.1.2 Polar UPLC-MS Method

Analytical characterization of hydrophilic, polar organic compounds was performed using an optimized UPLC gradient method. A Waters Acquity H-Class UPLC ® with TUV detector and QDa Mass spectrometer was utilized. Typically, 1µl injections were separated using an Acquity UPLC BEH C18 1.7 µm column (2.1 x 50mm) at 80°C. Eluent was monitored by UV (220 and 254nm), fluorescence (ex. 488nm, em. 520nm) and mass spectrometry (150-1250 Da, ES+/ES-). Solvents for the mobile phase were water with 0.1% formic acid (solvent A) and acetonitrile (ACN) with 0.1% formic acid (solvent B). Flow rate was 0.8 ml/min. Gradient Used: Isocratic solvent B for 1.0 min (0-1.0min), then gradient from 3% to 50% Solvent B over 2.0 min (1.0-3.0min), then gradient from 50% to 95% solvent B over 1.2 min (3.0-4.2min), then isocratic solvent B for 0.1 min (4.2-4.3min), then gradient from 95% to 3% solvent B for 0.1 min (4.3-4.4min), then isocratic solvent B for 0.6 min (4.4-5.0min) (Table II).

Table II. Solvent Gradient for Polar UPLC-MS Method

Time	Flow rate (mL/min)	%A	%B
Initial	0.80	97.0%	3.0%
1.00	0.80	97.0%	3.0%
3.00	0.80	50.0%	50.0%
4.20	0.80	5.0%	95.0%
4.30	0.80	5.0%	95.0%
4.40	0.80	97.0%	3.0%
5.00	0.80	97.0%	3.0%

5.1.3 Normal HPLC-MS Method

Analytical characterization of large (> 1250 Da) organic compounds was performed using a Waters Auto-purification system containing a 2545 binary gradient module, 2767 sample manager, 2998 UV/PDA detector, and SQD2 mass spectrometer. Typically, 1µl injections were separated using an XBridge BEH C18 5µm (4.6 x 100 mm) column at 80°C. Eluent was monitored by UV (210-600nm), and mass spectrometry (150-1800 Da, ES+/ES-). Solvents for the mobile phase were water with 0.05% formic acid (solvent A) and acetonitrile (ACN) with 0.05% formic acid (solvent B). Flow rate was 2.00 ml/min.

Gradient Used: Isocratic solvent B for 1.0 min (0-1.0 min), then gradient from 5% to 99% solvent B over 2.8 min (1.0-3.8min), then isocratic solvent B for 0.1 min (3.8-3.9min), then gradient from 99% to 5% solvent B for 0.1 min (3.9-4.0min), then isocratic solvent B for 1.0 min (4.0-5.0min) (Table III).

Table III. Solvent Gradient for Normal HPLC-MS Method

Time	Flow rate (mL/min)	%A	%B
Initial	2.00	95.0%	5.0%
1.00	2.00	95.0%	5.0%
3.80	2.00	1.0%	99.0%
3.90	2.00	1.0%	99.0%
4.00	2.00	95.0%	5.0%
5.00	2.00	95.0%	5.0%

5.2 Preparative HPLC Methods

5.2.1 Normal Preparative HPLC Method

General purification of organic compounds was performed using a Waters Auto-purification system containing a 2545 binary gradient module, 2767 sample manager, 2998 UV/PDA detector, and SQD2 mass spectrometer. Typically, 500µl injections were separated using an XBridge BEH C18 5 µm OBD (19 x 100 mm) prep column at room temperature. Eluent was monitored by UV (210-600nm), and mass spectrometry (150-2500 Da, ES+/ES-). Solvent for the mobile phase were water with 0.05% trifluoroacetic acid (solvent A) and acetonitrile (ACN) with 0.05% trifluoroacetic acid (solvent B). Flow rate was 20.0 ml/min. Gradient Used: Isocratic solvent B for 1.0 min (0-1.0min), then gradient from 15% to 95% solvent B over 7.0 min (1.0-8.0min), then isocratic solvent B for 0.5 min (8.0-8.5min), then gradient from 95% to 15% solvent B for 0.5 min (8.5-9.0min), then isocratic solvent B for 1.0 min (9.0-10.0min) (Table IV).

Table IV. Solvent Gradient for Normal Preparative HPLC Method

Time	Flow rate (mL/min)	%A	%B
Initial	20.0	85.0%	15.0%
1.00	20.0	85.0%	15.0%
8.00	20.0	5.0%	95.0%
8.50	20.0	5.0%	95.0%
9.00	20.0	85.0%	15.0%
10.00	20.0	85.0%	15.0%

5.2.2 Optimized Oregon Green Peptide Preparative HPLC Method

Purification of Oregon Green coupled linkers was optimized to separate closely eluting materials to product UV peaks that appeared under analytical traces. A Waters Auto-purification system containing a 2545 binary gradient module, 2767 sample manager, 2998 UV/PDA detector, and SQD2 mass spectrometer was employed. Typically, 500µl injections were separated using an XBridge BEH C18 5 µm OBD (19 x 100 mm) prep column at room temperature. Eluent was monitored by UV (210-600nm), and mass spectrometry (150-2500 Da, ES+/ES-). Solvents for the mobile phase were water with 0.05% trifluoroacetic acid (solvent A) and acetonitrile (ACN) with 0.05% trifluoroacetic acid (solvent B). Flow rate was 20.0 ml/min. Gradient Used: Isocratic solvent B for 1.0 min (0-1.0min), then gradient from 5% to 20% solvent B over 0.5 min (1.0-1.5min), then gradient from 20% to 50% solvent B over 7.5 min (1.5-8.0min), then gradient from 50% to 95% solvent B for 0.5 min (8.0-8.5min), then gradient from 95% to 5% solvent B for 0.5 min (8.5-9.0min), then isocratic solvent B for 1.0 min (9.0-10.0min) (Table V).

Table V. Solvent Gradient for Oregon Green Peptide Preparative HPLC Method

Time	Flow rate (mL/min)	%A	%B
Initial	20.0	95.0%	5.0%
1.00	20.0	95.0%	5.0%
1.50	20.0	80.0%	20.0%
8.00	20.0	50.0%	50.0%
8.50	20.0	5.0%	95.0%
9.00	20.0	95.0%	5.0%
10.00	20.0	95.0%	5.0%

5.3 Synthesis of p-amino benzylamide Oregon Green

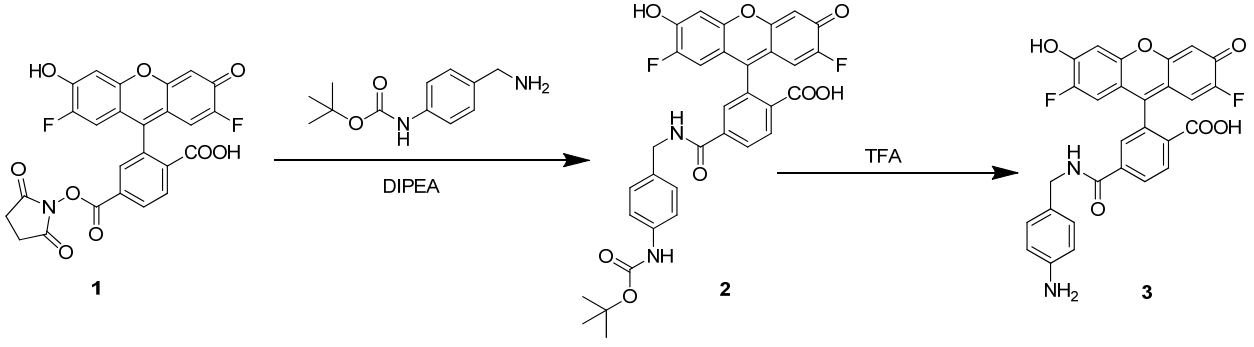

Oregon Green N-hydroxysuccimide ester **(1)** (48.7mg, 95.6 µmol, 1 equiv), 4-boc-amino benzylamine (34.5mg, 155 µmol, 1.6 equiv), and DIPEA (64mg, 490µmol, 5.1 equiv), was combined in anhydrous DMF at a reaction molarity of 50 mM for 4 hours at rt. The resulting 4-boc-aminobenzylamide Oregon Green **(2)** was confirmed through LC/MS (ESI): $(M+H)^+$ 617.2 Da, Retention time 3.47 min. Solution was concentrated to dryness over 12 hours. The resulting orange resin was deprotected without an intermediate purification step.

The orange resin **(2)** (95.6 µmol, 1 equiv) was dissolved into a 20% TFA in DCM solution at a reaction molarity of 50 mM for one hour at rt. The resulting p-aminobenzylamide Oregon Green **(3)** was confirmed through Fluorescence (ex. 488, em 520) and LC/MS (ESI): $(M+H)^+$ 517.2 Da, Retention time: 2.55 min (Figure S1, S2). Solution was concentrated to dryness, then dissolved into DMA for purification through the normal preparative HPLC to yield a yellow resin. Total recovery after two steps was 55.7mg (88.3 µmol, 92.4%). This yellow resin was again dissolved into DMA to make a 100 mM stock solution for future reactions using sub-milligram weights.

5.4 Synthesis of TAMRA-Mal-AEEA-Gly-P_2-P_1-p-aminobenzylamide-Oregon Green

Amide coupling of p-amino benzylamide Oregon Green to the C-terminus of purchased peptide linkers (Wuxi®) was dependent on the amino acid residues present. General conditions were used for all peptides except those containing lysine or histidine. Optimized conditions for histidine-containing linkers and lysine containing linkers are described separately.

5.4.1 Amide Coupling of PABA-Oregon Green to Mal-AEEA-Gly-P_2-P_1-OH

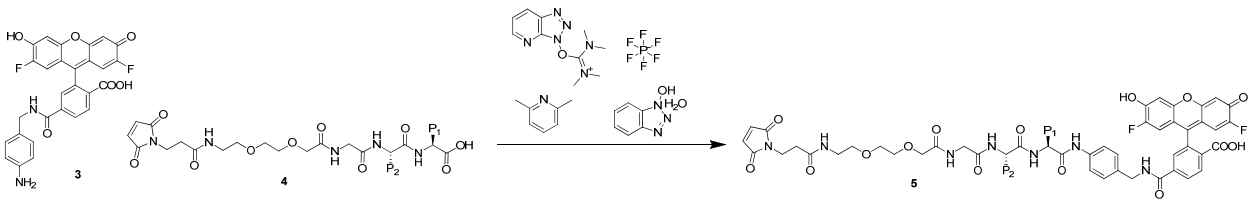

All purchased linkers **(4)** were made into 20mM stock solutions in DMA to measure sub-milligram quantities and the aniline **(3)** was previously made into a stock solution for the same reason. p-amino

benzylamide Oregon Green **(3)** (630 µg, 1.00µmol, 1equiv), linker Mal-AEEA-Gly-P_2-P_1-OH **(4)** (884 µg, 1.5µmol, 1.5 equiv) (Table S2), HATU (1.52mg, 4.00 µmol, 4 equiv), HOBt (153 µg, 1.00µmol, 1 equiv), and 2,6-Lutidine (426 µg, 4.00 µmol, 4 equiv) were combined in sufficient DMA to give a reaction molarity of 6.9 mM. The reaction was allowed to stand for 16 hours at rt. Product **(5)** formation was verified by LC/MS and purified by preparative HPLC using the optimized peptide prep method. The final amount of purified product **(5)** was determined using fluorescent quantitation against a standard curve prepared with p-amino benzylamide Oregon Green. Analytical characterization (ESI, retention time) under the polar UPLC analytical method, and reaction results (purity, yield) are reported in table S2. The resulting linker-fluorophores **(5)** were dissolved into DMA yielding a 50µM Stock solution for future use.

5.4.2 Amide Coupling of PABA-Oregon Green to Mal-AEEA-Gly-His-P_1-OH

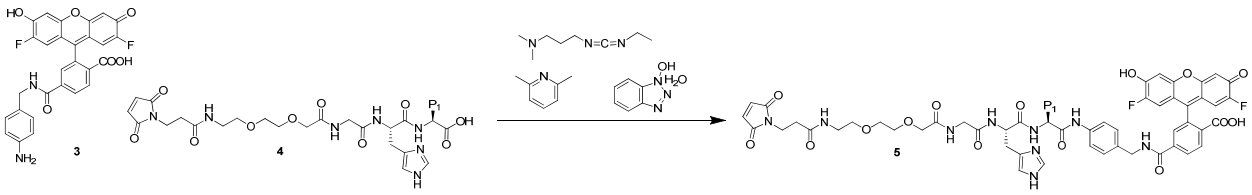

All purchased linkers **(4)** were made into 20mM stock solutions in DMA to measure sub-milligram quantities and the aniline **(3)** was previously made into a stock solution for the same reason. p-amino benzylamide Oregon Green (470 µg, 0.75 µmol, 1 equiv), linker Mal-AEEA-Gly-His-P_1-OH (1.3 mg, 2.3µmol, 3 equiv) (Table S3), EDC (580 µg, 3.00 µmol, 4 equiv), HOBt (460 µg, 3.00µmol, 4 equiv), and 2,6-Lutidine (320 µg, 3.00 µmol, 4 equiv) were combined in DMA for a reaction molarity of 4.5 mM for 16 hours at rt. Product formation was verified by LC/MS and purified through preparative HPLC using the optimized peptide prep method. Analytical characterization (ESI, retention time) under the polar UPLC analytical method, and reaction results (purity, yield) are reported in table S3. The resulting linker-fluorophores **(5)** were dissolved into DMA yielding a 50µM Stock solution for future use.

5.4.3 Amide Coupling of PABA-Oregon Green to Mal-AEEA-Gly-P_2-His-OH

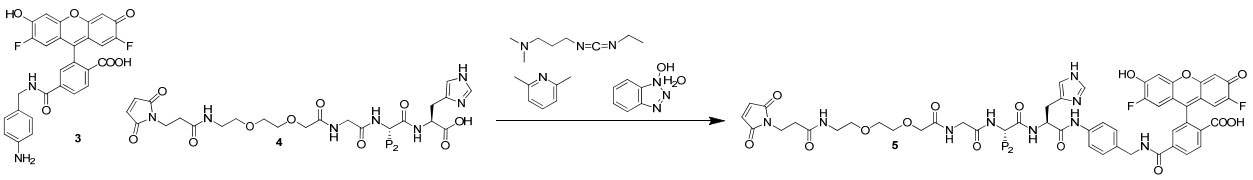

All purchased linkers **(4)** were made into 20mM stock solutions in DMA to measure sub-milligram quantities and the aniline **(3)** was previously made into a stock solution for the same reason. p-amino benzylamide Oregon Green **(3)** (470 µg, 0.75 µmol, 1 equiv), linker Mal-AEEA-Gly-P_2-His-OH **(4)** (1.3 mg, 2.3µmol, 3 equiv) (Table S4), EDC (580 µg, 3.00 µmol, 4 equiv), HOBt (460 µg, 3.00µmol, 4 equiv), and 2,6-Lutidine (320 µg, 3.00 µmol, 4 equiv) were combined in DMA for a reaction molarity of 4.5 mM for 16 hours at rt. Product **(5)** formation was verified by LC/MS and purified through preparative HPLC using the optimized peptide prep method. Analytical characterization (ESI, retention time) under the polar UPLC analytical method, and reaction results (purity, yield) are reported in table S4. The resulting linker-fluorophores **(5)** were dissolved into DMA yielding a 50µM Stock solution for future use.

5.4.4 Amide Coupling of PABA-Oregon Green to Mal-AEEA-Gly-P_2-Lys-OH

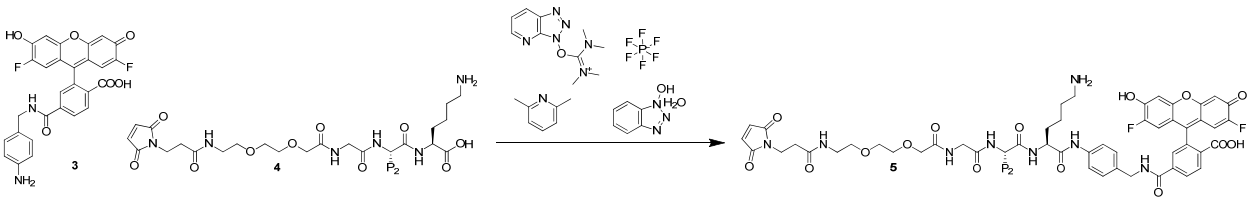

All purchased linkers **(4)** were made into 20mM stock solutions in DMA to measure sub-milligram quantities and the aniline **(3)** was previously made into a stock solution for the same reason. p-amino benzylamide Oregon Green **(3)** (1.89 mg, 3.00 µmol, 3 equiv), linker Mal-AEEA-Gly-P_2-Lys-OH **(4)** (590 µg, 1.0 µmol, 1 equiv) (Table S5), HATU (1.52mg, 4.00 µmol, 4 equiv), HOBt (153 µg, 1.00µmol, 1 equiv), and 2,6-Lutidine (426 µg, 4.00 µmol, 4 equiv) were combined in DMA for a reaction molarity of 6.9 mM for 16 hours at rt. Product **(5)** formation was verified by LC/MS and purified through preparative HPLC using the optimized peptide prep method. Analytical characterization (ESI, retention time) under the polar UPLC analytical method, and reaction results (purity, yield) are reported in table S5.

The resulting linker-fluorophores **(5)** were dissolved into DMA yielding a 50µM Stock solution for future use.

5.4.5 Michael Addition of TAMRA thiol to Mal-AEEA-Gly-P_2-P_1-PABA-OG

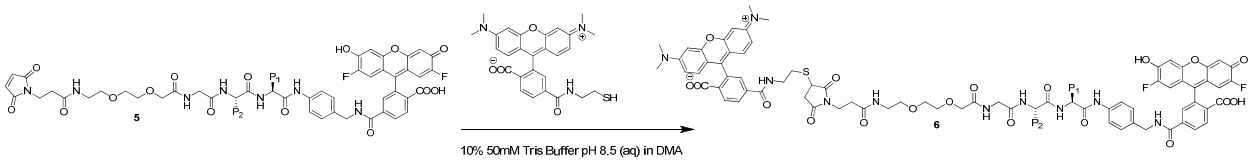

All linker-fluorophores **(5)** were previously made into 50µM stock solutions in DMA to measure sub-milligram quantities and TAMRA-thiol was made into a 150µM stock solution in DMA for the purpose of the Michael Addition. Mal-AEEA-Gly-P_2-P_1-PABA-OG (**5)** (50µl, 2.5 nmol, 1 equiv) and TAMRA thiol (50µl, 12.5 nmol, 5 equiv) was combined into a solution of DMA and 50 mM Tris pH 8.5 buffer (aq) (10% by volume) for a reaction molarity of 23 µM for 2 hours at rt. The kinetics of the Michael Addition were tracked to ensure a complete thiolation of the maleimide was achieved (Fig. 6). Fluorescence of Oregon Green was tracked over time to monitor the decrease in fluorescence post-thiol addition. The thiol was shown to consume most thiol within the first minute of exposure, with negligible change after one hour. Therefore, this reaction was run for two hours to ensure complete consumption of the maleimide.

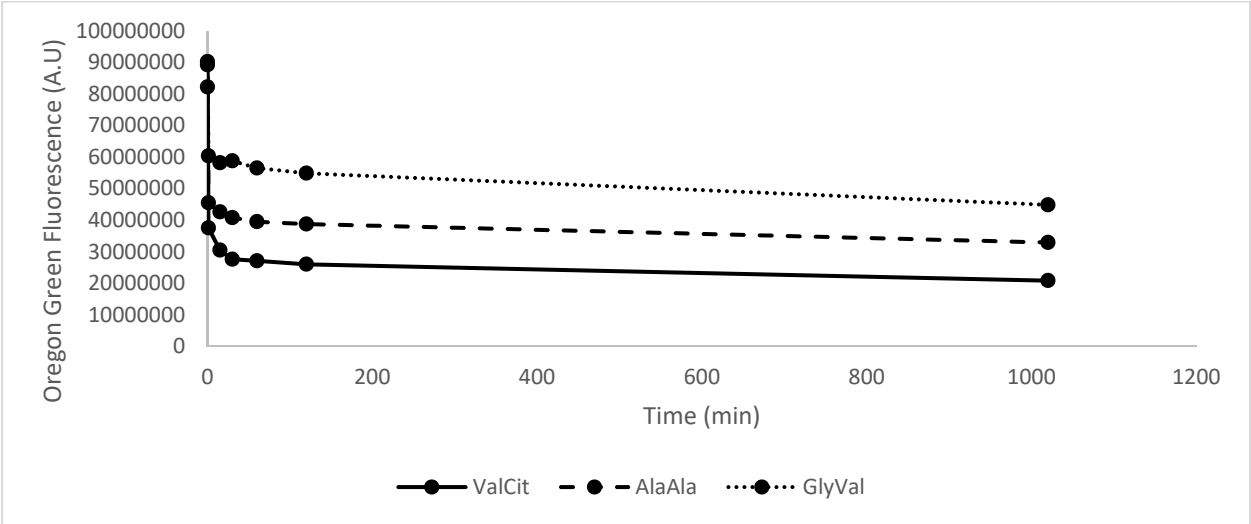

Figure 7. Michael addition of TAMRA-thiol to the N-terminal maleimide fluorescence kinetics

Product formation **(6)** was confirmed quantitatively through the change in Oregon Green fluorescence. For each FRET pair prepared *in situ,* TAMRA-Mal-AEEA-Gly-P_2-P_1-PABA-OG **(6)** (4.4µl, 0.10 nmol) was diluted in 195.6 µl of 5.6% DMA in NaOAc buffer (pH 5.2) yielding a 200µl, 500 nM solution. For each linker, a standard 500nM solution of Mal-AEEA-Gly-P_2-P_1-PABA-OG **(6)** was prepared for comparison by diluting Mal-AEEA-Gly-P_2-P_1-PABA-OG **(6)** (2.0µl, 0.10 nmol) into 198.0µl of 6.7% DMA in NaOAc buffer (pH 5.2). Fluorescence of Oregon Green within TAMRA-Mal-AEEA-Gly-P_2-P_1-PABA-OG **(6)** and the control Mal-AEEA-Gly-P_2-P_1-PABA-OG **(5)** was measured at excitation 488nm and emission 520nm and the concentration of Oregon Green was back-calculated using a linear standard curve. Percent difference in fluorescence is reported in table S1.

5.5 Synthesis of Mal-AEEA-Gly-P2-P1-PABC-MMAE Linker Payloads

5.5.1 Amide Coupling of p-amino benzyl alcohol to Mal-AEEA-Gly-P2-P1-OH

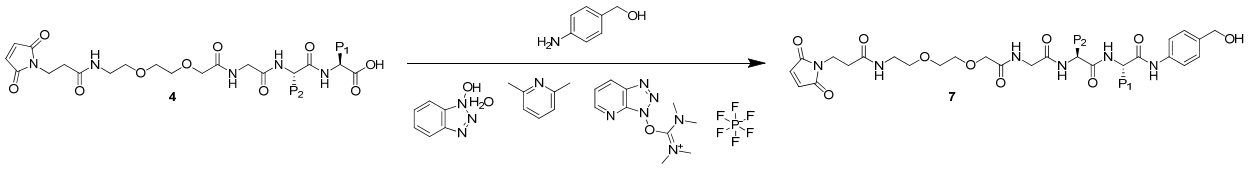

Mal-AEEA-Gly-P1-P2-OH **(4)** (8.35 mg, 15.0 µmol, 1 equiv), p-aminobenzyl alcohol (2.77mg, 22.5µmol, 1.5 equiv), HATU (22.8mg, 60.0 µmol, 4 equiv), HOBt (2.30 mg, 15.0 µmol, 1 equiv), and 2,6-Lutidine (6.4mg, 60.0µmol, 4 equiv) were combined in DMA for a reaction molarity of 13.0 mM for 2 hours at rt. Product **(7)** formation was verified by LC/MS, and purified through the optimized peptide prep method. Resulting alcohols **(7)** were green resins. Analytical characterization (ESI, retention time) under the polar UPLC analytical method, and reaction results (purity, yield) are reported in table S6.

5.5.2 Activation of Benzyl Alcohol with Bis-p-nitrophenyl Carbonate

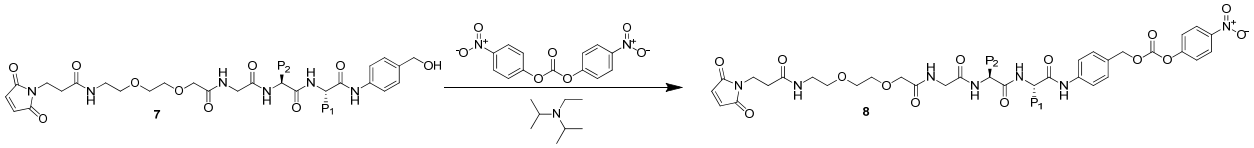

Mal-AEEA-Gly-P1-P2-PAB-OH **(7)** (Table S8, 1 equiv), bis-p-nitrophenyl carbonate (Table S9, 1.75 equiv), and DIPEA (Table S9, 1.5 equiv) were combined in anhydrous DMF for 24 hours at rt. Product **(8)** formation was verified by LC/MS using the normal UPLC analytical method (Table S7). The material was moved forward without a purification step.

5.5.3 Substitution of p-nitrophenyl with Monomethyl Auristatin E (MMAE)

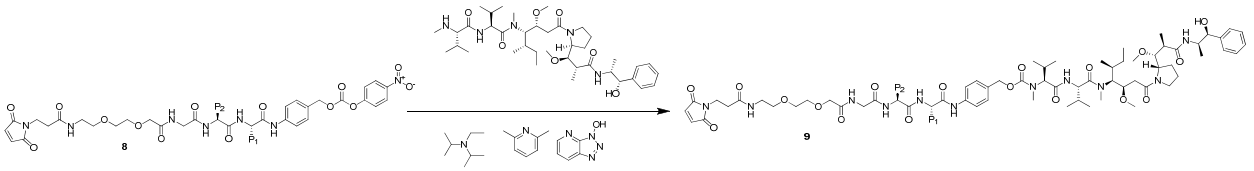

Mal-AEEA-Gly-P1-P2-PABC-PNP **(8)** (Table S10, 1 equiv), MMAE (Table S10, 2 equiv), HOAt (Table S10, 1 equiv), 2,6-Lutidine (Table S10, 2 equiv), and DIPEA (Table S10, 3 equiv) were combined in the anhydrous DMF of the previous reaction, and left at rt for 48 hours. Product **(9)** formation was verified by LC/MS and purified by preparative HPLC using the normal preparative method. Resulting products were a clear resin. Analytical characterization (ESI, retention time) under the normal HPLC analytical method and reaction results (purity, total yield over two steps) are reported on table S8.

5.6 *In vitro* Enzymatic Stability Assays

5.6.1 Cathepsin B Stability Assay

Human Liver Cathepsin B was purchased from MilliporeSigma. Cathepsin B was activated using DTT by combining 67.5µl of cathepsin B (1mg/ml) with 67.5µl of DTT (50mM) in NaOAc (0.2M, pH 5.2) and heating the solution at 37°C for 20 minutes. Activated cathepsin B (0.5 mg/ml) was diluted using 240µl of NaOAc (0.2M, pH 5.2) yielding an 80 µg/ml enzyme concentration. FRET pairs prepared *in situ* were plated by combining TAMRA-Mal-AEEA-Gly-P2-P1-PABA-OG (4.4µl 0.10 nmol), 190.6µl of 5.75%

DMA in NaOAc buffer (0.2M, pH 5.2) and activated cathepsin B (5µl, 400 ng) for a final linker concentration of 500nM and final enzyme concentration of 2 µg/ml in Aqueous 7.5% DMA in NaOAc (0.2M, pH 5.2) buffer. The assay was performed in a 96-well plate format at ambient temperature. Change in Oregon Green fluorescence was measured at excitation 488nm and emission 520nm over 12 hours taking a timepoint every 10 minutes. Data analysis is described below.

5.6.2 Tritosomal Stability Assay

Rat liver tritosomes were purchased from XenoTech. Tritosomes were activated using DTT by combining 230µl of tritosomes (2.5mg/ml) with 230µl of DTT (50mM) in NaOAc (0.2M, pH 4.7) and heating the solution at 37°C for 30 minutes. Activated tritosomes (1.25 mg/ml) were diluted using 1070µl of NaOAc (0.2M, pH 4.7) yielding a 375 µg/ml enzyme concentration. FRET pairs prepared *in situ* were plated in a 96-well plate by combining TAMRA-Mal-AEEA-Gly-P2-P1-PABA-OG **(6)** (4.4µl 0.10 nmol), 175.6µl of 5.75% DMA in NaOAc buffer (0.2M, pH 4.7) and activated tritosomes (20µl, 7.50 µg) for a final linker concentration of 500nM and final enzyme concentration of 37.5 µg/ml in Aqueous 7.5% DMA in NaOAc (0.2M, pH 4.7) buffer. The assay was performed in a 96-well plate format at ambient temperature. Change in Oregon Green fluorescence was measured at excitation 488nm and emission 520nm over 6.5 hours taking a timepoint every 10 minutes using a Molecular Devices i3x Microplate Reader. Data analysis is described below.

5.6.3 Legumain Stability Assay

Recombinant human legumain was purchased from Novoprotein Scientific. Legumain was activated using DTT by combining 43µl of tritosomes (1.0mg/ml) with 43µl of DTT (50mM) in NaOAc (0.2M, pH 4.7) and heating the solution at 37°C for 30 minutes. Activated legumain (0.50 mg/ml) was diluted using 730µl of NaOAc(0.2M, pH 4.7) yielding a 50 µg/ml enzyme concentration. FRET pairs prepared *in situ* were plated in a 96-well plate by combining TAMRA-Mal-AEEA-Gly-P2-P1-PABA-OG **(6)** (2.2µl, 0.5 nmol), 87.8µl of NaOAc buffer (pH 4.7) and activated legumain (10µl, 500 ng) for a linker concentration of 500 nM and enzyme concentration of 5.0 µg/ml in aqueous 2.0% DMA in NaOAc (pH 4.7) buffer. The

assay was performed in a 96-well plate format at ambient temperature. Change in Oregon Green fluorescence was measured at excitation 488nm and emission 520nm over 12 hours taking a timepoint every 10 minutes using a Molecular Devices i3x Microplate Reader. Data analysis is described below.

5.6.4 Carboxyesterase 1C Stability Assay

Recombinant mouse carboxyesterase 1C was purchased from MyBioSource. Enzyme was prepared by diluting 80.5µl of Ces1C (1 mg/ml) with 724.5 µl of PBS (0.01M, pH 7.4) yielding a 100 µg/ml enzyme concentration. FRET pairs were prepared *in situ* were plated in a 96-well plate by combining TAMRA-Mal-AEEA-Gly-P2-P1-PABA-OG **(6)** (2.2µl, 0.05 nmol), 87.8µl of PBS buffer (0.01M, pH 7.4) and Ces1C (10µl, 1.0 µg) for a final linker concentration of 500 nM and final enzyme concentration of 10 µg/ml in Aqueous 2.0% DMA in PBS (0.01M, pH 7.4) buffer. The assay was performed in a 96-well plate format at 37°C. Change in Oregon Green fluorescence was measured at excitation 488nm and emission 520nm over 10 days taking a timepoint once every 24 hours using a Molecular Devices i3x Microplate Reader. Data analysis is described below.

5.6.5 Quantitative Analysis of Single Enzyme FRET Pair Hydrolysis

5.6.5.1 Calculating Percent Cleavage of the Peptide Linker

Cathepsin B, tritosomes, legumain and Ces1C activity on each peptide linker was evaluated by calculating the final percent cleavage of each linker. Fluorescence readings were converted to molarity through a linear Oregon Green standard curve spanning 7.8 nM to 1000 nM, a subsection of the shown linear range (Fig. 8). Taking the initial and final timepoint, percent cleavage was calculated through the following equation:

$$Percent\ Cleavage = \frac{Final\ Molarity - Initial\ Molarity}{Theoredical\ Maximim\ Molarity - Initial\ Molarity}$$

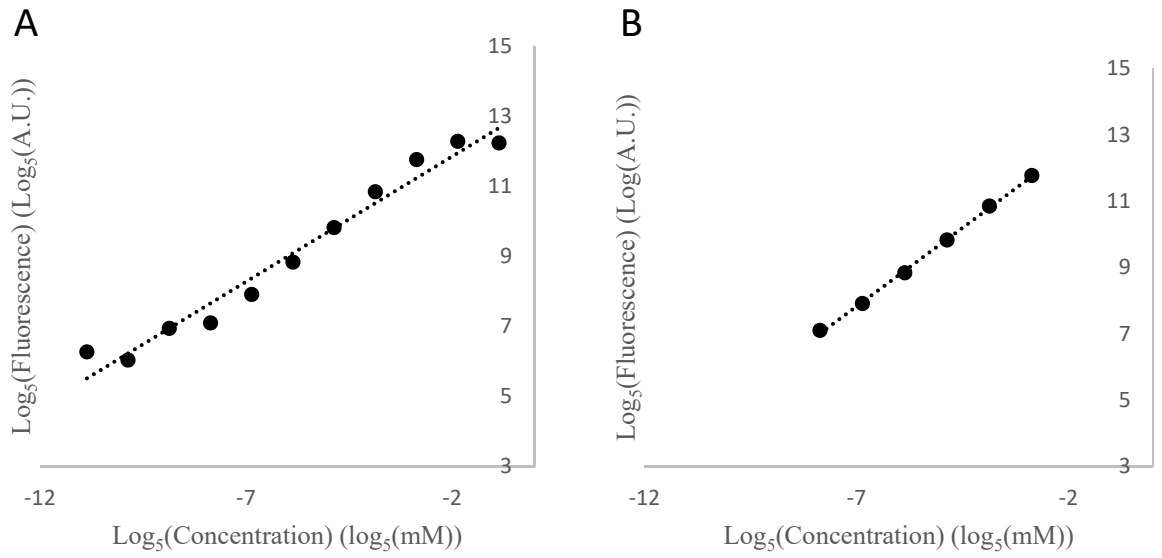

Figure 8. Oregon Green fluorescent Standard curves. Double log was taken to show linearity from 128pM to 50µM. A) Fluorescence of Oregon Green over 128pM to 50µM. R = 0.9675 B) Linear portion of figure 8A. Linearity was shown to range from 3.2nM to 10µM. R = 0.9989

5.6.5.2 Calculating Enzymatic Velocity of Peptide Linker Hydrolysis

Cathepsin B, tritosomes, legumain and Ces1C activity on each peptide linker was evaluated by calculating the initial enzymatic velocity. Initial enzymatic velocity was calculated by taking the derivative of the linear region of the plot moles of Oregon green vs. time. This linear region was found to be the first 10% of cleavage for peptides of positive velocities under all enzymatic conditions. For a peptide exceeding 10% cleavage, the slope of the linear region was calculated from time zero until the timepoint exceeding 10% cleavage. For a peptide less than 10% cleavage, the slope of was calculated for all timepoints. Correlation coefficients (R) were calculated for each regression to verify linearity (Table S11).

5.7 *In vitro* Serum Stability Assays

5.7.1 Mouse Serum Stability Assay

Mouse serum was purchased from Equitech-Bio. Mouse serum was prepared through filter sterilization and followed by combining penicillin (100µl, 100 units) with mouse serum (10 ml). FRET pairs prepared *in situ* were plated by plating TAMRA-Mal-AEEA-Gly-P2-P1-PABA-OG **(6)** (4.4 µl 0.10 nmol), 195.4µl

of sterile mouse serum for a linker concentration of 500 nM and DMA percent volume of 2.0%. Change in Oregon Green fluorescence was measured at excitation 488nm and emission 520nm over 18 hours taking a timepoint once every 10 minutes using a Molecular Devices i3x Microplate Reader. Data analysis is described below.

5.7.2 Human Serum Stability Assay

Human serum was purchased from MP Biomedicals. Human serum was prepared through filter sterilization by combining penicillin (100µl, 100 units) with human serum (10 ml). FRET pairs prepared *in situ* were plated by plating TAMRA-Mal-AEEA-Gly-P2-P1-PABA-OG **(6)** (4.4 µl 0.10 nmol), 195.4µl of sterile human serum for a linker concentration of 500 nM and DMA percent volume of 2.0%. Change in Oregon Green fluorescence was measured at excitation 488nm and emission 520nm over 18 hours taking a timepoint once every 10 minutes using a Molecular Devices i3x Microplate Reader. Data analysis is described below.

5.7.3 Quantitative Analysis of Linker Serum Stability

Activity of enzymes on each peptide linker within mouse and human serum was evaluated by calculating the final percent cleavage of each linker. Fluorescence readings were converted to molarity through a linear Oregon Green Standard curve spanning 7.8 nM to 1000 nM (Fig. 8). Taking the initial and final timepoint, percent cleavage was calculated through the following equation:

$$Percent\ Cleavage = \frac{Final\ Molarity - Initial\ Molarity}{Theoredical\ Maximim\ Molarity - Initial\ Molarity}$$

6 Supplemental Material

6.1 Percent Oregon Green Signal Quenching of FRET Pairs

Table S1. Percent Oregon Green Fluorescence Signal Quenching of FRET Pairs upon addition of the TAMRA-thiol.

FRET Pair Chemistry (P_2-P_1)	Percent OG Signal Quenched (%)
TAMRA-3-Mal-AEEA-Gly-Val-Cit-PABA-OG	83.3
TAMRA-3-Mal-AEEA-Gly-D-Val-D-Cit-PABA-OG	74.6
TAMRA-3-Mal-AEEA-Gly-Ala-Ala-PABA-OG	54.0
TAMRA-3-Mal-AEEA-Gly-Gly-Gly-PABA-OG	77.0
TAMRA-3-Mal-AEEA-Gly-Gly-Asn-PABA-OG	61.5
TAMRA-3-Mal-AEEA-Gly-Gly-Aib-PABA-OG	48.5
TAMRA-3-Mal-AEEA-Gly-Gly-1nal-PABA-OG	78.8
TAMRA-3-Mal-AEEA-Gly-Gly-2nal-PABA-OG	76.4
TAMRA-3-Mal-AEEA-Gly-Gly-Phe-PABA-OG	36.9
TAMRA-3-Mal-AEEA-Gly-Gly-His-PABA-OG	74.7
TAMRA-3-Mal-AEEA-Gly-Gly-Val-PABA-OG	37.7
TAMRA-3-Mal-AEEA-Gly-Gly-Lys-PABA-OG	36.6
TAMRA-3-Mal-AEEA-Gly-Gly-Cit-PABA-OG	40.6
TAMRA-3-Mal-AEEA-Gly-Gly-Trp-PABA-OG	42.5
TAMRA-3-Mal-AEEA-Gly-Ser-Asn-PABA-OG	86.3
TAMRA-3-Mal-AEEA-Gly-Ser-Aib-PABA-OG	84.9
TAMRA-3-Mal-AEEA-Gly-Ser-Phe-PABA-OG	67.7
TAMRA-3-Mal-AEEA-Gly-Ser-His-PABA-OG	54.9
TAMRA-3-Mal-AEEA-Gly-Ser-Ala-PABA-OG	77.5
TAMRA-3-Mal-AEEA-Gly-Ser-Val-PABA-OG	70.8
TAMRA-3-Mal-AEEA-Gly-Ser-Lys-PABA-OG	28.1
TAMRA-3-Mal-AEEA-Gly-Ser-Cit-PABA-OG	84.5
TAMRA-3-Mal-AEEA-Gly-Ser-Trp-PABA-OG	83.6
TAMRA-3-Mal-AEEA-Gly-Pro-Asn-PABA-OG	75.2
TAMRA-3-Mal-AEEA-Gly-Pro-Aib-PABA-OG	57.1
TAMRA-3-Mal-AEEA-Gly-Pro-Phe-PABA-OG	75.0
TAMRA-3-Mal-AEEA-Gly-Pro-His-PABA-OG	84.8
TAMRA-3-Mal-AEEA-Gly-Pro-Ala-PABA-OG	76.9
TAMRA-3-Mal-AEEA-Gly-Pro-Val-PABA-OG	86.9
TAMRA-3-Mal-AEEA-Gly-Pro-Lys-PABA-OG	71.1
TAMRA-3-Mal-AEEA-Gly-Pro-Cit-PABA-OG	77.2
TAMRA-3-Mal-AEEA-Gly-Pro-Trp-PABA-OG	83.9
TAMRA-3-Mal-AEEA-Gly-His-Asn-PABA-OG	83.5
TAMRA-3-Mal-AEEA-Gly-His-Aib-PABA-OG	77.0
TAMRA-3-Mal-AEEA-Gly-His-Phe-PABA-OG	71.4
TAMRA-3-Mal-AEEA-Gly-His-Ala-PABA-OG	70.3
TAMRA-3-Mal-AEEA-Gly-His-Val-PABA-OG	75.2
TAMRA-3-Mal-AEEA-Gly-His-Cit-PABA-OG	69.8

TAMRA-3-Mal-AEEA-Gly-His-Trp-PABA-OG	74.7
TAMRA-3-Mal-AEEA-Gly-Tyr-Asn-PABA-OG	86.8
TAMRA-3-Mal-AEEA-Gly-Tyr-Aib-PABA-OG	85.2
TAMRA-3-Mal-AEEA-Gly-Tyr-Phe-PABA-OG	74.2
TAMRA-3-Mal-AEEA-Gly-Tyr-Phe-PABA-OG	82.6
TAMRA-3-Mal-AEEA-Gly-Tyr-Ala-PABA-OG	78.5
TAMRA-3-Mal-AEEA-Gly-Tyr-Val-PABA-OG	72.7
TAMRA-3-Mal-AEEA-Gly-Tyr-Lys-PABA-OG	25.0
TAMRA-3-Mal-AEEA-Gly-Tyr-Cit-PABA-OG	70.0
TAMRA-3-Mal-AEEA-Gly-Tyr-Trp-PABA-OG	84.7
TAMRA-3-Mal-AEEA-Gly-Gln-Asn-PABA-OG	89.2
TAMRA-3-Mal-AEEA-Gly-Gln-Aib-PABA-OG	79.8
TAMRA-3-Mal-AEEA-Gly-Gln-Phe-PABA-OG	81.5
TAMRA-3-Mal-AEEA-Gly-Gln-His-PABA-OG	87.0
TAMRA-3-Mal-AEEA-Gly-Gln-Ala-PABA-OG	57.1
TAMRA-3-Mal-AEEA-Gly-Gln-Val-PABA-OG	57.5
TAMRA-3-Mal-AEEA-Gly-Gln-Lys-PABA-OG	43.8
TAMRA-3-Mal-AEEA-Gly-Gln-Cit-PABA-OG	83.8
TAMRA-3-Mal-AEEA-Gly-Gln-Trp-PABA-OG	88.1
TAMRA-3-Mal-AEEA-Gly-Ile-Asn-PABA-OG	79.9
TAMRA-3-Mal-AEEA-Gly-Ile-Aib-PABA-OG	92.3
TAMRA-3-Mal-AEEA-Gly-Ile-Phe-PABA-OG	78.3
TAMRA-3-Mal-AEEA-Gly-Ile-His-PABA-OG	83.6
TAMRA-3-Mal-AEEA-Gly-Ile-Ala-PABA-OG	91.8
TAMRA-3-Mal-AEEA-Gly-Ile-Val-PABA-OG	93.9
TAMRA-3-Mal-AEEA-Gly-Ile-Lys-PABA-OG	38.6
TAMRA-3-Mal-AEEA-Gly-Ile-Cit-PABA-OG	88.6
TAMRA-3-Mal-AEEA-Gly-Ile-Trp-PABA-OG	87.2
TAMRA-3-Mal-AEEA-Gly-Asn-Asn-PABA-OG	88.7
TAMRA-3-Mal-AEEA-Gly-Asn-Aib-PABA-OG	87.3
TAMRA-3-Mal-AEEA-Gly-Asn-Phe-PABA-OG	87.1
TAMRA-3-Mal-AEEA-Gly-Asn-His-PABA-OG	85.0
TAMRA-3-Mal-AEEA-Gly-Asn-Ala-PABA-OG	71.5
TAMRA-3-Mal-AEEA-Gly-Asn-Val-PABA-OG	81.6
TAMRA-3-Mal-AEEA-Gly-Asn-Lys-PABA-OG	80.5
TAMRA-3-Mal-AEEA-Gly-Asn-Cit-PABA-OG	90.9
TAMRA-3-Mal-AEEA-Gly-Asn-Trp-PABA-OG	93.1

6.2 Analytical Characterization of Organic Compounds

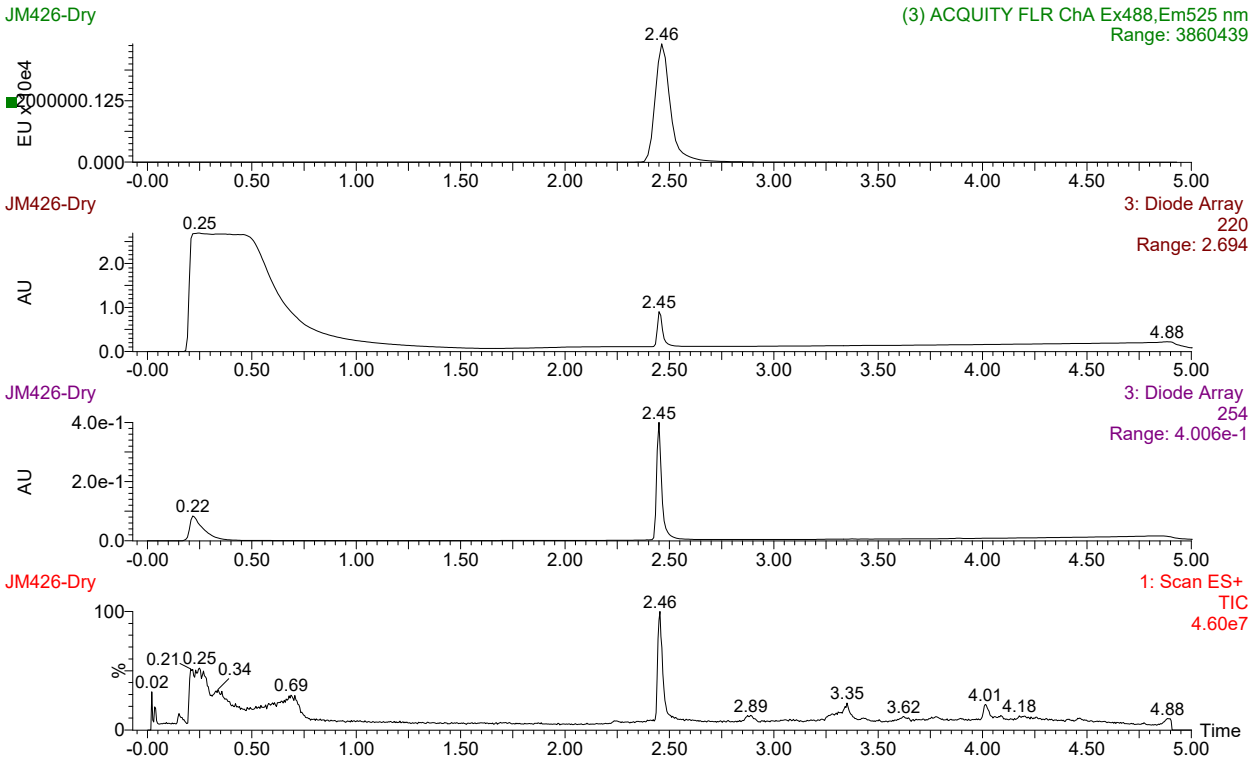

Figure S1. Analytical Characterization of Modified Oregon Green Fluorophore. Fluorescence (ex. 488nm, em. 520nm), UV absorbance at 220 and 254nm, and mass spectrometry of Purified fluorophore are displayed.

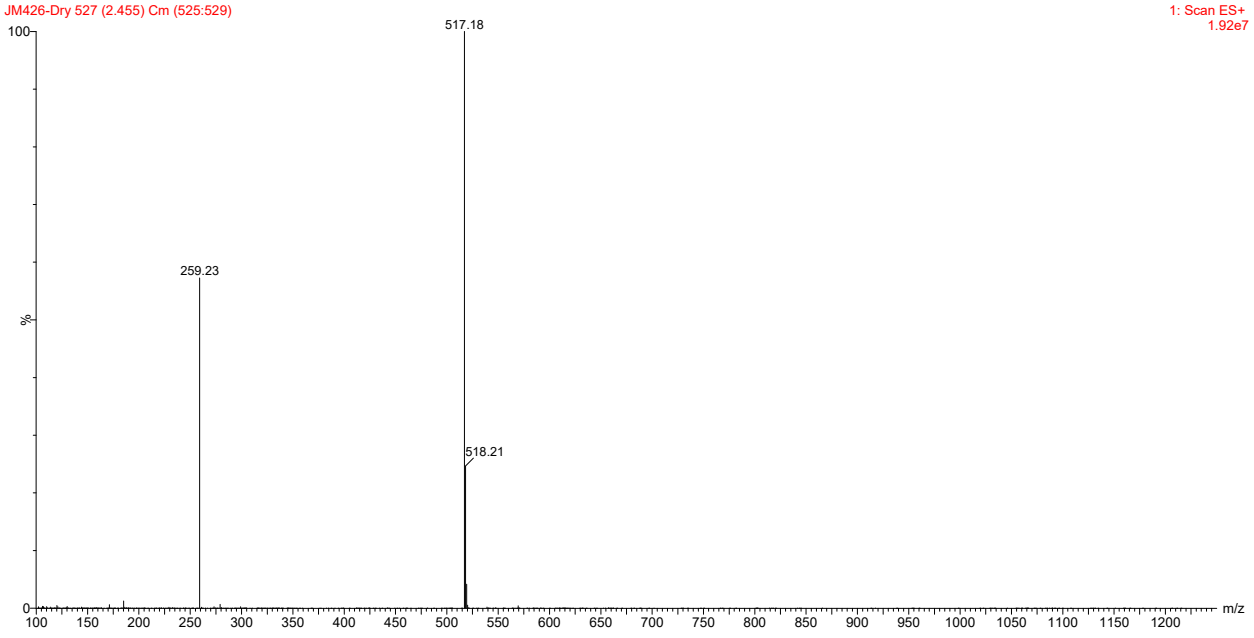

Figure S2. Mass spectrometry of Modified Oregon Green Fluorophore (m.w. = 516.2 Da)

Table S2. Analytical Characterization and Reaction Results of Mal-AEEA-Gly-P_2-P_1-p-aminobenzyl amide Oregon Green Synthesis.

Product Linker Chemistry (3-Mal-AEEA-Gly-P2-P1-PABA-OG)	ESI: $(M+H)^+$	Retention Time (min)	Mass Recovered (mg)	Percent Yield (%)	HPLC Purity
3-Mal-AEEA-Gly-Val-Cit-PABA-OG	1126.53	2.91	0.072	6.41	>99%
3-Mal-AEEA-Gly-D-Val-D-Cit-PABA-OG	1126.56	2.90	0.156	13.79	>99%
3-Mal-AEEA-Gly-Ala-Ala-PABA-OG	1012.43	2.88	0.186	18.38	>99%
3-Mal-AEEA-Gly-Gly-Gly-PABA-OG	984-.39	2.80	0.247	20.60	>95%
3-Mal-AEEA-Gly-Gly-Asn-PABA-OG	1041.47	2.75	0.062	4.85	>99%
3-Mal-AEEA-Gly-Gly-Aib-PABA-OG	1012.40	2.88	0.044	3.56	~60%
3-Mal-AEEA-Gly-Gly-1nal-PABA-OG	1124.48	3.28	0.213	15.52	>99%
3-Mal-AEEA-Gly-Gly-2nal-PABA-OG	1124.51	3.30	0.163	11.92	>99%
3-Mal-AEEA-Gly-Gly-Phe-PABA-OG	1074.52	3.11	0.131	10.03	~65%
3-Mal-AEEA-Gly-Gly-Val-PABA-OG	1026.49	3.00	0.121	9.71	~65%
3-Mal-AEEA-Gly-Gly-Cit-PABA-OG	1084.47	2.76	0.133	10.05	~75%
3-Mal-AEEA-Gly-Gly-Trp-PABA-OG	1113.51	3.11	0.084	6.19	~80%
3-Mal-AEEA-Gly-Ser-Asn-PABA-OG	1071.45	2.75	0.126	9.65	>99%
3-Mal-AEEA-Gly-Ser-Aib-PABA-OG	1042.46	2.86	0.167	13.20	>99%
3-Mal-AEEA-Gly-Ser-Phe-PABA-OG	1104.55	3.10	0.547	40.73	>95%
3-Mal-AEEA-Gly-Ser-Ala-PABA-OG	1028.44	2.83	0.273	21.78	>99%
3-Mal-AEEA-Gly-Ser-Val-PABA-OG	1056.53	2.96	0.366	28.48	>99%
3-Mal-AEEA-Gly-Ser-Cit-PABA-OG	1114.55	2.75	0.266	19.58	>99%
3-Mal-AEEA-Gly-Ser-Trp-PABA-OG	1143.52	3.09	0.312	22.42	>99%
3-Mal-AEEA-Gly-Pro-Asn-PABA-OG	1081.50	2.81	0.171	12.97	>92%
3-Mal-AEEA-Gly-Pro-Aib-PABA-OG	1052.51	2.86	0.149	11.66	>60%
3-Mal-AEEA-Gly-Pro-Phe-PABA-OG	1114.54	3.21	0.367	27.05	>95%
3-Mal-AEEA-Gly-Pro-Ala-PABA-OG	1038.46	2.91	0.389	30.79	>92%
3-Mal-AEEA-Gly-Pro-Val-PABA-OG	1066.50	3.06	0.361	27.80	>99%
3-Mal-AEEA-Gly-Pro-Cit-PABA-OG	1124.53	2.83	0.290	21.21	>92%
3-Mal-AEEA-Gly-Pro-Trp-PABA-OG	1153.50	3.18	0.245	17.43	>99%
3-Mal-AEEA-Gly-Tyr-Asn-PABA-OG	1147.48	2.85	0.164	11.75	>99%
3-Mal-AEEA-Gly-Tyr-Aib-PABA-OG	1118.51	3.00	0.072	5.29	>99%
3-Mal-AEEA-Gly-Tyr-Phe-PABA-OG	1180.50	3.20	0.282	19.63	>90%
3-Mal-AEEA-Gly-Tyr-Ala-PABA-OG	1104.48	2.95	0.320	23.82	>99%
3-Mal-AEEA-Gly-Tyr-Val-PABA-OG	1132.53	3.06	0.241	17.46	>90%
3-Mal-AEEA-Gly-Tyr-Cit-PABA-OG	1190.91	2.86	0.256	17.67	>90%
3-Mal-AEEA-Gly-Tyr-Trp-PABA-OG	1219.45	3.18	0.195	13.15	>99%
3-Mal-AEEA-Gly-Gln-Asn-PABA-OG	1112.54	2.73	0.130	9.57	>99%
3-Mal-AEEA-Gly-Gln-Aib-PABA-OG	1083.51	2.85	0.099	7.54	>95%
3-Mal-AEEA-Gly-Gln-Phe-PABA-OG	1145.52	3.06	0.305	21.87	>99%
3-Mal-AEEA-Gly-Gln-Ala-PABA-OG	1069.45	2.81	0.471	36.16	>92%
3-Mal-AEEA-Gly-Gln-Val-PABA-OG	1097.52	2.93	0.449	33.63	>80%
3-Mal-AEEA-Gly-Gln-Cit-PABA-OG	1155.48	2.73	0.287	20.40	>99%
3-Mal-AEEA-Gly-Gln-Trp-PABA-OG	1184.46	3.06	0.072	5.02	>99%
3-Mal-AEEA-Gly-Ile-Asn-PABA-OG	1097.51	2.95	0.116	8.67	>95%

3-Mal-AEEA-Gly-Ile-Aib-PABA-OG	1068.57	3.13	0.114	11.13	>99%
3-Mal-AEEA-Gly-Ile-Phe-PABA-OG	1130.57	3.33	0.240	17.44	>95%
3-Mal-AEEA-Gly-Ile-Ala-PABA-OG	1054.48	3.06	0.293	22.82	>99%
3-Mal-AEEA-Gly-Ile-Val-PABA-OG	1082.55	3.20	0.236	17.89	>99%
3-Mal-AEEA-Gly-Ile-Cit-PABA-OG	1140.51	2.96	0.163	11.71	>99%
3-Mal-AEEA-Gly-Ile-Trp-PABA-OG	1169.53	3.30	0.140	9.81	>99%
3-Mal-AEEA-Gly-Asn-Asn-PABA-OG	1098.47	2.73	0.165	12.32	>99%
3-Mal-AEEA-Gly-Asn-Aib-PABA-OG	1069.46	2.83	0.188	14.45	>95%
3-Mal-AEEA-Gly-Asn-Phe-PABA-OG	1131.49	3.05	0.348	25.24	>99%
3-Mal-AEEA-Gly-Asn-Ala-PABA-OG	1055.53	2.81	0.200	15.61	>85%
3-Mal-AEEA-Gly-Asn-Val-PABA-OG	1083.51	2.93	0.218	16.52	>99%
3-Mal-AEEA-Gly-Asn-Cit-PABA-OG	1141.46	2.73	0.536	38.60	>99%
3-Mal-AEEA-Gly-Asn-Trp-PABA-OG	1170.50	3.05	0.218	15.32	>99%

Table S3. Analytical Characterization and Reaction Results of Mal-AEEA-Gly-His-P_1-p-aminobenzyl amide Oregon Green Synthesis.

Product Linker Chemistry (3-Mal-AEEA-Gly-P_2-P_1-PABA-OG)	ESI: $(M+H)^+$	Retention Time (min)	Mass Recovered (mg)	Percent Yield (%)	HPLC Purity
3-Mal-AEEA-Gly-His-Asn-PABA-OG	1121.53	2.48	0.152	14.83	>99%
3-Mal-AEEA-Gly-His-Aib-PABA-OG	1092.53	2.56	0.037	3.68	>99%
3-Mal-AEEA-Gly-His-Phe-PABA-OG	1154.51	2.75	0.048	4.52	>99%
3-Mal-AEEA-Gly-His-Ala-PABA-OG	1078.51	2.55	0.058	5.90	>99%
3-Mal-AEEA-Gly-His-Val-PABA-OG	1106.53	2.85	0.042	4.20	>99%
3-Mal-AEEA-Gly-His-Cit-PABA-OG	1164.55	2.48	0.031	2.92	>99%
3-Mal-AEEA-Gly-His-Trp-PABA-OG	1193.50	2.76	0.039	3.58	>99%

Table S4. Analytical Characterization and Reaction Results of Mal-AEEA-Gly-P_2-His- p-aminobenzyl amide Oregon Green Synthesis.

Product Linker Chemistry (3-Mal-AEEA-Gly-P_2-P_1-PABA-OG)	ESI: $(M+H)^+$	Retention Time (min)	Mass Recovered (mg)	Percent Yield (%)	HPLC Purity
3-Mal-AEEA-Gly-Gly-His-PABA-OG	1064.50	2.50	0.137	10.54	>99%
3-Mal-AEEA-Gly-Ser-His-PABA-OG	1094.53	2.50	0.082	8.47	>99%
3-Mal-AEEA-Gly-Pro-His-PABA-OG	1104.47	2.55	0.182	18.18	>99%
3-Mal-AEEA-Gly-Tyr-His-PABA-OG	1170.50	2.58	0.144	14.28	>99%
3-Mal-AEEA-Gly-Gln-His-PABA-OG	1135.51	2.48	0.213	19.97	>99%
3-Mal-AEEA-Gly-Ile-His-PABA-OG	1120.53	2.66	0.102	9.86	>99%
3-Mal-AEEA-Gly-Asn-His-PABA-OG	1121.51	2.48	0.119	11.65	>99%

Table S5. Analytical Characterization and Reaction Results of Mal-AEEA-Gly-P_2-Lys- p-aminobenzyl amide Oregon Green Synthesis.

Product Linker Chemistry (3-Mal-AEEA-Gly-P_2-P_1-PABA-OG)	ESI: $(M+H)^+$	Retention Time (min)	Mass Recovered (mg)	Percent Yield (%)	HPLC Purity
3-Mal-AEEA-Gly-Gly-Lys-PABA-OG	1055.55	2.50	0.120	9.30	>99%
3-Mal-AEEA-Gly-Ser-Lys-PABA-OG	1085.61	2.50	0.009	0.70	>70%
3-Mal-AEEA-Gly-Pro-Lys-PABA-OG	1095.59	2.55	0.102	7.64	>99%
3-Mal-AEEA-Gly-Tyr-Lys-PABA-OG	1161.11	2.51	0.338	23.93	>50%
3-Mal-AEEA-Gly-Gln-Lys-PABA-OG	1126.52	2.46	0.137	9.99	>99%
3-Mal-AEEA-Gly-Ile-Lys-PABA-OG	1111.58	2.70	0.208	15.36	>60%
3-Mal-AEEA-Gly-Asn-Lys-PABA-OG	1112.56	2.46	0.164	12.14	>99%

Table S6. Analytical Characterization and Reaction Results of Mal-AEEA-Gly-P_2-P_1-PAB-OH Synthesis.

Product Linker Chemistry (3-Mal-AEEA-Gly-P_2-P_1-PAB-OH)	ESI: $(M+H)^+$	Retention Time (min)	Mass Recovered (mg)	Percent Yield (%)	HPLC Purity
3-Mal-AEEA-Gly-Val-Cit-PAB-OH	733.3	2.36	9.5	86.4	>99%
3-Mal-AEEA-Gly-Ser-Asn-PAB-OH	678.3	2.07	5.9	58.1	>99%
3-Mal-AEEA-Gly-Tyr-Trp-PAB-OH	826.3	2.79	9.7	78.4	>99%
3-Mal-AEEA-Gly-Gln-Asn-PAB-OH	719.2	2.08	7.4	68.7	>99%
3-Mal-AEEA-Gly-Gln-Val-PAB-OH	704.3	2.42	9.2	87.2	>99%
3-Mal-AEEA-Gly-Asn-Asn-PAB-OH	705.3	2.05	8.5	80.4	>99%
3-Mal-AEEA-Gly-Asn-Ala-PAB-OH	662.3	2.18	5.5	55.4	>99%

Table S7. Analytical Characterization and Results of Mal-AEEA-Gly-P_2-P_1-PABC-PNP Synthesis

Product Linker Chemistry (3-Mal-AEEA-Gly-P_2-P_1-PABC-PNP)	ESI: $(M+H)^+$	Retention Time (min)	Theoretical Mass (mg)	Theoretical Moles (µmol)
3-Mal-AEEA-Gly-Val-Cit-PABC-PNP	898.3	2.74	11.6	13.0
3-Mal-AEEA-Gly-Ser-Asn-PABC-PNP	843.2	2.45	7.3	8.7
3-Mal-AEEA-Gly-Tyr-Trp-PABC-PNP	991.3	2.99	11.6	11.8
3-Mal-AEEA-Gly-Gln-Asn-PABC-PNP	884.3	2.45	9.1	10.3
3-Mal-AEEA-Gly-Gln-Val-PABC-PNP	869.3	2.78	11.4	13.1
3-Mal-AEEA-Gly-Asn-Asn-PABC-PNP	870.2	2.44	10.5	12.1
3-Mal-AEEA-Gly-Asn-Ala-PABC-PNP	827.3	2.59	6.9	8.3

Table S8. Analytical Characterization and Results of Mal-AEEA-Gly-P_2-P_1-PABC-MMAE Synthesis.

Product Linker Chemistry (3-Mal-AEEA-Gly-P_2-P_1-PABC-MMAE)	ESI: $(M+H)^+$	Retention Time (min)	Mass Recovered(mg)	Percent Yield (%)	HPLC Purity
3-Mal-AEEA-Gly-Val-Cit-PABC-MMAE	1477.4	3.41	1.1	5.7	> 99%
3-Mal-AEEA-Gly-Ser-Asn-PABC-MMAE	1422.4	3.40	0.8	6.5	< 50%
3-Mal-AEEA-Gly-Tyr-Trp-PABC-MMAE	1570.5	3.57	1.7	9.2	>93%
3-Mal-AEEA-Gly-Gln-Asn-PABC-MMAE	1463.5	3.31	2.9	19.2	> 99%
3-Mal-AEEA-Gly-Gln-Val-PABC-MMAE	1448.4	3.45	1.7	9.0	> 99%
3-Mal-AEEA-Gly-Asn-Asn-PABC-MMAE	1449.3	3.32	4.0	22.9	> 99%

3-Mal-AEEA-Gly-Asn-Ala-PABC-MMAE	1406.4	3.38	2.3	19.7	> 99%

6.3 Reaction Conditions of MMAE Linker Payload Synthesis

Table S9. Reaction Conditions and Results of Mal-AEEA-Gly-P_2-P_1-PABC-PNP Synthesis.

Product Linker Chemistry (3-Mal-AEEA-Gly-P_2-P_1-PABC-PNP)	Mass Bis-PNP-Carbonate (mg)	Mole Bis-PNP-Carbonate (µmol)	Mass DIPEA (mg)	Mole DIPEA (µmol)
3-Mal-AEEA-Gly-Val-Cit-PABC-PNP	6.90	21.4	2.5	19.5
3-Mal-AEEA-Gly-Ser-Asn-PABC-PNP	4.63	13.5	1.7	13.1
3-Mal-AEEA-Gly-Tyr-Trp-PABC-PNP	6.25	19.4	2.3	17.6
3-Mal-AEEA-Gly-Gln-Asn-PABC-PNP	5.48	16.1	2.0	15.5
3-Mal-AEEA-Gly-Gln-Val-PABC-PNP	6.96	24.7	2.5	19.6
3-Mal-AEEA-Gly-Asn-Asn-PABC-PNP	6.42	20.7	2.3	18.1
3-Mal-AEEA-Gly-Asn-Ala-PABC-PNP	4.43	14.8	1.6	12.5

Table S10. Reaction Conditions of Mal-AEEA-Gly-P_2-P_1-PABC-MMAE Synthesis.

Product Linker Chemistry (3-Mal-AEEA-Gly-P_2-P_1-PABC-MMAE)	Mass MMAE (mg)	Mole MMAE (µmol)	Mass HOAt (mg)	Mole HOAt (µmol)
3-Mal-AEEA-Gly-Val-Cit-MMAE	17.20	24.0	1.8	13.0
3-Mal-AEEA-Gly-Ser-Asn-MMAE	10.93	15.2	1.2	8.7
3-Mal-AEEA-Gly-Tyr-Trp-PABC-MMAE	15.61	21.8	1.6	11.8
3-Mal-AEEA-Gly-Gln-Asn-PABC-MMAE	13.04	18.2	1.4	10.3
3-Mal-AEEA-Gly-Gln-Val-PABC-MMAE	19.58	27.3	1.8	13.1
3-Mal-AEEA-Gly-Asn-Asn-PABC-MMAE	16.60	23.1	1.6	12.1
3-Mal-AEEA-Gly-Asn-Ala-PABC-MMAE	11.81	16.5	1.1	8.3
Product Linker Chemistry (3-Mal-AEEA-Gly-P_2-P_1-PABC-MMAE)	Mass DIPEA (mg)	Mole DIPEA (µmol)	Mass 2,6-Lutidine (mg)	Mole 2,6-Lutidine (µmol)
3-Mal-AEEA-Gly-Val-Cit-PABC-MMAE	5.0	38.9	2.8	25.9
3-Mal-AEEA-Gly-Ser-Asn-PABC-MMAE	3.4	26.1	1.9	17.4
3-Mal-AEEA-Gly-Tyr-Trp-PABC-MMAE	4.6	35.3	2.5	23.5
3-Mal-AEEA-Gly-Gln-Asn-PABC-MMAE	4.0	30.9	2.2	20.6
3-Mal-AEEA-Gly-Gln-Val-PABC-MMAE	5.1	39.2	2.8	26.2
3-Mal-AEEA-Gly-Asn-Asn-PABC-MMAE	4.7	36.2	2.6	24.1
3-Mal-AEEA-Gly-Asn-Ala-PABC-MMAE	3.2	25.0	1.8	16.6

6.4 Regression Analysis of Initial Enzymatic Velocities

Table S11. Initial Enzymatic Velocities and Regression Analysis of Catabolic Enzymes against Linkers

	Cathepsin B		Tritosomes		Legumain		Ces1C	
Linker Chemistry (P_2-P_1)	V_0 (nmol/min)	R	V_0 (nmol/min)	R	V_0 (nmol/min)	R	V_0 (nmol/min)	R
ValCit	5.82E-05	0.999	6.62E-05	0.999	8.39E-07	0.959	1.78E-05	0.936
D-Val-D-Cit	5.69E-06	0.962	8.82E-06	0.949	1.19E-06	0.906	2.22E-05	0.980
AlaAla	2.76E-05	0.977	2.64E-05	0.949	2.01E-06	0.849	3.83E-05	0.974
GlyGly	6.35E-06	0.986	8.69E-06	0.943	1.39E-06	0.904	0.000193	0.999
GlyAsn	8.66E-06	0.989	1.26E-05	0.947	1.06E-06	0.790	0.000147	1.000
GlyAib	1.06E-05	0.966	1.3E-05	0.893	1.81E-06	0.836	0.000124	0.994
Gly1nal	7.69E-06	0.985	8.34E-06	0.933	2.94E-06	0.862	0.00019	0.998
Gly2nal	7.97E-06	0.986	7.11E-06	0.916	2.94E-06	0.826	0.000226	0.979
GlyPhe	7.58E-06	0.926	1.26E-05	0.850	1.29E-05	0.931	0.000121	1.000
GlyHis	4.52E-06	0.975	6.71E-06	0.904	6.25E-07	0.797	3.39E-05	0.939
GlyVal	9.22E-06	0.906	1.35E-05	0.871	2.36E-06	0.797	9.26E-05	0.980
GlyLys	1.42E-05	0.941	3.92E-05	0.965	8.59E-07	0.618	-4.7E-06	-0.300
GlyCit	1.03E-05	0.941	1.25E-05	0.866	2.09E-06	0.791	7.75E-05	0.964
GlyTrp	6.74E-06	0.873	4.47E-06	0.515	2.5E-06	0.619	2.04E-05	0.928
SerAsn	3.53E-06	0.968	4.32E-05	0.998	1.02E-05	0.994	7.73E-05	0.989
SerAib	1.88E-06	0.932	3.28E-06	0.867	3.52E-07	0.572	6.32E-05	0.996
SerPhe	1.86E-06	0.886	2.75E-06	0.637	9.99E-07	0.813	2.84E-05	0.982
SerHis	-9.6E-07	-0.292	-2.5E-06	-0.558	1.15E-06	0.917	4.53E-05	0.947
SerAla	1.07E-05	0.996	6.77E-06	0.895	8.19E-07	0.906	7.16E-05	0.963
SerVal	6.08E-07	0.418	1.19E-06	0.396	5.44E-07	0.873	3.32E-05	0.986
SerLys	-2.7E-06	-0.388	-6.7E-06	-0.650	6.16E-07	0.525	2.59E-05	0.972
SerCit	7.94E-06	0.993	8.21E-06	0.958	5.84E-07	0.889	5.93E-05	0.990
SerTrp	6.76E-06	0.994	5.12E-06	0.951	7.33E-07	0.941	0.000272	1.000
ProAsn	4.36E-06	0.990	9.28E-06	0.944	1.21E-06	0.945	6.76E-05	0.998
ProAib	2.52E-06	0.826	6.54E-06	0.880	3.36E-07	0.685	3.77E-05	0.975
ProPhe	2.25E-06	0.957	2.88E-06	0.734	1.07E-06	0.899	5.24E-05	0.964
ProHis	1.92E-06	0.912	2.74E-06	0.763	8.07E-07	0.953	6.92E-05	0.950
ProAla	2.61E-06	0.948	3.31E-06	0.782	6.01E-07	0.917	4.34E-05	0.986
ProVal	2.72E-07	0.315	1.95E-06	0.736	4.9E-07	0.844	3.09E-05	0.984
ProLys	4.16E-07	0.307	-1.5E-06	-0.448	9.62E-07	0.921	4.74E-05	0.981
ProCit	1.14E-06	0.805	2.55E-06	0.728	8.08E-07	0.925	3.38E-05	0.980
ProTrp	3.45E-06	0.958	6.79E-06	0.941	1.46E-06	0.939	0.000398	1.000
HisAsn	5.87E-07	0.589	3.32E-06	0.861	1.36E-06	0.980	5.39E-05	0.994
HisAib	3.45E-07	0.395	5.03E-07	0.196	7.02E-07	0.880	5.43E-05	0.989
HisPhe	1.97E-06	0.877	1.02E-06	0.272	1.7E-06	0.891	4.04E-05	0.973
HisAla	7.55E-06	0.990	5.69E-06	0.860	7.16E-07	0.905	2.52E-05	0.930
HisVal	4.74E-06	0.986	4.65E-06	0.837	1.54E-06	0.894	2.28E-05	0.948
HisCit	3.01E-06	0.967	3.87E-07	0.157	7.62E-07	0.928	1.39E-05	0.967
HisTrp	2.76E-06	0.937	1.21E-06	0.407	1.39E-06	0.858	0.000198	1.000
TyrAsn	5.3E-06	0.988	3E-05	0.994	6.16E-06	0.996	6.04E-05	0.984

TyrAib	3.82E-07	0.445	2.01E-06	0.613	7.64E-07	0.848	8.49E-05	0.994
TyrPhe	4.61E-06	0.989	8.16E-05	0.999	1.67E-06	0.856	4.66E-05	0.981
TyrPhe	7.3E-06	0.973	2.14E-05	0.984	1.21E-06	0.880	3.77E-05	0.969
TyrAla	4.15E-05	0.999	5.54E-05	0.996	6.89E-07	0.870	3.53E-05	0.985
TyrVal	-1E-06	-0.557	6.34E-06	0.853	9.01E-07	0.885	2.13E-05	0.970
TyrLys	1.86E-06	0.420	3.65E-06	0.374	9.67E-07	0.614	7.85E-06	0.965
TyrCit	2.91E-05	0.995	5.34E-05	0.996	8.63E-07	0.906	2.76E-05	0.983
TyrTrp	1.77E-05	0.997	0.000164	0.999	1.52E-06	0.925	0.000476	1.000
GlnAsn	4.47E-06	0.970	2.13E-05	0.997	5.45E-06	0.992	5.73E-05	0.995
GlnAib	1.46E-06	0.881	2.31E-06	0.707	8.15E-07	0.936	7E-05	0.997
GlnPhe	2.39E-06	0.919	4.68E-06	0.883	9.27E-07	0.889	4.16E-05	0.994
GlnHis	1.72E-06	0.909	2.38E-06	0.728	9.47E-07	0.938	5.83E-05	0.956
GlnAla	8.25E-07	0.392	-1.8E-07	-0.041	5.1E-07	0.831	3.74E-05	0.964
GlnVal	-4.9E-06	-0.911	-4.3E-06	-0.736	9.99E-07	0.896	1.41E-05	0.969
GlnLys	-1E-05	-0.877	-1.8E-05	-0.938	1.84E-06	0.829	4.75E-05	0.966
GlnCit	2.99E-06	0.920	5.95E-06	0.787	7.69E-07	0.891	3.15E-05	0.982
GlnTrp	3.72E-06	0.971	6.07E-06	0.949	1.11E-06	0.972	9.25E-05	0.935
IleAsn	6.33E-06	0.985	4.19E-05	0.996	1.3E-05	0.986	8.27E-05	0.998
IleAib	2.19E-06	0.881	5.65E-06	0.945	6.39E-07	0.956	6.04E-05	0.994
IlePhe	1.62E-05	0.991	2.54E-05	0.984	2.58E-06	0.912	9.81E-05	0.972
IleHis	5.06E-06	0.935	7.06E-06	0.962	9.58E-07	0.928	5.89E-05	0.942
IleAla	5.38E-05	0.990	4.43E-05	0.998	5.55E-07	0.939	4.97E-05	0.991
IleVal	2.12E-06	0.861	5.02E-06	0.958	5.57E-07	0.897	4.52E-05	0.989
IleLys	1.31E-06	0.159	-9E-06	-0.775	1.61E-06	0.841	4.98E-05	0.924
IleCit	3.09E-05	0.993	3.94E-05	0.993	6.65E-07	0.842	6.68E-05	0.997
IleTrp	1.28E-05	0.993	3.58E-05	0.998	1.38E-06	0.901	0.000458	1.000
AsnAsn	2.78E-07	0.371	0.000325	1.000	9.34E-05	0.997	8.45E-05	1.000
AsnAib	-4.6E-07	-0.524	1.43E-06	0.559	6.3E-07	0.936	7.56E-05	0.997
AsnPhe	1.96E-06	0.941	0.000272	0.999	4.62E-05	0.993	5.8E-05	0.994
AsnHis	3.27E-06	0.977	0.00011	1.000	1.92E-05	0.998	5.53E-05	0.991
AsnAla	1.27E-05	0.981	0.000284	0.999	6.32E-05	0.996	5.66E-05	0.993
AsnVal	2.22E-06	0.948	0.000124	0.999	4.8E-05	0.996	2.01E-05	0.869
AsnLys	8.83E-06	0.957	0.000137	0.998	2.71E-05	0.997	6.19E-05	0.976
AsnCit	8.18E-06	0.966	0.000152	1.000	3.8E-05	0.997	2.98E-05	0.970
AsnTrp	8.16E-06	0.977	0.000227	1.000	2.73E-05	0.995	0.00025	1.000

7 References

(1) Bae, Y. H.; Park, K. Targeted Drug Delivery to Tumors: Myths, Reality and Possibility. *J. Control. Release* **2011**, *153* (3), 198–205. https://doi.org/10.1016/j.jconrel.2011.06.001.

(2) Parslow, A. C.; Parakh, S.; Lee, F.-T.; Gan, H. K.; Scott, A. M. Antibody-Drug Conjugates for Cancer Therapy. *Biomedicines* **2016**, *4* (3), 14. https://doi.org/10.3390/biomedicines4030014.

(3) Sandall, S. L.; McCormick, R.; Miyamoto, J.; Biechele, T.; Law, C.-L.; Lewis, T. S. Abstract 946: SGN-CD70A, a Pyrrolobenzodiazepine (PBD) Dimer Linked ADC, Mediates DNA Damage Pathway Activation and G2 Cell Cycle Arrest Leading to Cell Death. *Cancer Res.* **2015**, *75* (15 Supplement), 946 LP – 946. https://doi.org/10.1158/1538-7445.AM2015-946.

(4) Menderes, G.; Bonazzoli, E.; Bellone, S.; Black, J.; Altwerger, G.; Masserdotti, A.; Pettinella, F.; Zammataro, L.; Buza, N.; Hui, P.; et al. SYD985, a Novel Duocarmycin-Based HER2-Targeting Antibody-Drug Conjugate, Shows Promising Antitumor Activity in Epithelial Ovarian Carcinoma with HER2/Neu Expression. *Gynecol. Oncol.* **2017**, *146* (1), 179–186. https://doi.org/10.1016/j.ygyno.2017.04.023.

(5) Gerber, H.-P.; Kung-Sutherland, M.; Stone, I.; Morris-Tilden, C.; Miyamoto, J.; McCormick, R.; Alley, S. C.; Okeley, N.; Hayes, B.; Hernandez-Ilizaliturri, F. J.; et al. Potent Antitumor Activity of the Anti-CD19 Auristatin Antibody Drug Conjugate HBU12-VcMMAE against Rituximab-Sensitive and -Resistant Lymphomas. *Blood* **2009**, *113* (18), 4352–4361. https://doi.org/10.1182/blood-2008-09-179143.

(6) Tannir, N. M.; Forero-Torres, A.; Ramchandren, R.; Pal, S. K.; Ansell, S. M.; Infante, J. R.; de Vos, S.; Hamlin, P. A.; Kim, S. K.; Whiting, N. C.; et al. Phase I Dose-Escalation Study of SGN-75 in Patients with CD70-Positive Relapsed/Refractory Non-Hodgkin Lymphoma or Metastatic Renal Cell Carcinoma. *Invest. New Drugs* **2014**, *32* (6), 1246–1257. https://doi.org/10.1007/s10637-014-0151-0.

(7) Lewis Phillips, G. D.; Li, G.; Dugger, D. L.; Crocker, L. M.; Parsons, K. L.; Mai, E.; Blättler, W. A.; Lambert, J. M.; Chari, R. V. J.; Lutz, R. J.; et al. Targeting HER2-Positive Breast Cancer with Trastuzumab-DM1, an Antibody–Cytotoxic Drug Conjugate. *Cancer Res.* **2008**, *68* (22), 9280 LP – 9290. https://doi.org/10.1158/0008-5472.CAN-08-1776.

(8) Liu, C.; Sun, C.; Huang, H.; Janda, K.; Edgington, T. Overexpression of Legumain in Tumors Is Significant for Invasion/Metastasis and a Candidate Enzymatic Target for Prodrug Therapy. *Cancer Res.* **2003**, *63* (11), 2957 LP – 2964.

(9) Nejadmoghaddam, M.-R.; Minai-Tehrani, A.; Ghahremanzadeh, R.; Mahmoudi, M.; Dinarvand, R.; Zarnani, A.-H. Antibody-Drug Conjugates: Possibilities and Challenges. *Avicenna J. Med. Biotechnol.* **2019**, *11* (1), 3–23.

(10) Tsuchikama, K.; An, Z. Antibody-Drug Conjugates: Recent Advances in Conjugation and Linker Chemistries. *Protein Cell* **2018**, *9* (1), 33–46. https://doi.org/10.1007/s13238-016-0323-0.

(11) Katz, J.; Janik, J. E.; Younes, A. Brentuximab Vedotin (SGN-35). *Clin. Cancer Res.* **2011**, *17* (20), 6428 LP – 6436. https://doi.org/10.1158/1078-0432.CCR-11-0488.

(12) Palanca-Wessels, M. C. A.; Czuczman, M.; Salles, G.; Assouline, S.; Sehn, L. H.; Flinn, I.; Patel, M. R.; Sangha, R.; Hagenbeek, A.; Advani, R.; et al. Safety and Activity of the Anti-CD79B Antibody–Drug Conjugate Polatuzumab Vedotin in Relapsed or Refractory B-Cell Non-Hodgkin Lymphoma and Chronic Lymphocytic Leukaemia: A Phase 1 Study. *Lancet Oncol.* **2015**,

16 (6), 704–715. https://doi.org/10.1016/S1470-2045(15)70128-2.

(13) Dorywalska, M.; Dushin, R.; Moine, L.; Farias, S. E.; Zhou, D.; Navaratnam, T.; Lui, V.; Hasa-Moreno, A.; Casas, M. G.; Tran, T.-T.; et al. Molecular Basis of Valine-Citrulline-PABC Linker Instability in Site-Specific ADCs and Its Mitigation by Linker Design. *Mol. Cancer Ther.* **2016**, *15* (5), 958 LP – 970. https://doi.org/10.1158/1535-7163.MCT-15-1004.

(14) Ubink, R.; Dirksen, E. H. C.; Rouwette, M.; Bos, E. S.; Janssen, I.; Egging, D. F.; Loosveld, E. M.; van Achterberg, T. A.; Berentsen, K.; van der Lee, M. M. C.; et al. Unraveling the Interaction between Carboxylesterase 1c and the Antibody–Drug Conjugate SYD985: Improved Translational PK/PD by Using Ces1c Knockout Mice. *Mol. Cancer Ther.* **2018**, *17* (11), 2389 LP – 2398. https://doi.org/10.1158/1535-7163.MCT-18-0329.

(15) Strop, P.; Liu, S. H.; Dorywalska, M.; Delaria, K.; Dushin, R. G.; Tran, T. T.; Ho, W. H.; Farias, S.; Casas, M. G.; Abdiche, Y.; et al. Location Matters: Site of Conjugation Modulates Stability and Pharmacokinetics of Antibody Drug Conjugates. *Chem. Biol.* **2013**, *20* (2), 161–167. https://doi.org/10.1016/j.chembiol.2013.01.010.

(16) Dorywalska, M.; Strop, P.; A. Melton-Witt, J.; Hasa-Moreno, A.; E. Farias, S.; Galindo Casas, M.; Delaria, K.; Lui, V.; Poulsen, K.; Loo, C.; et al. Effect of Attachment Site on Stability of Cleavable Antibody Drug Conjugates. *Bioconjug. Chem.* **2015**, *26* (4), 650–659. https://doi.org/10.1021/bc5005747.

(17) Zhao, H.; Gulesserian, S.; Malinao, M. C.; Ganesan, S. K.; Song, J.; Chang, M. S.; Williams, M. M.; Zeng, Z.; Mattie, M.; Mendelsohn, B. A.; et al. A Potential Mechanism for ADC-Induced Neutropenia: Role of Neutrophils in Their Own Demise. *Mol. Cancer Ther.* **2017**, *16* (9), 1866 LP – 1876. https://doi.org/10.1158/1535-7163.MCT-17-0133.

(18) Anami, Y.; Yamazaki, C. M.; Xiong, W.; Gui, X.; Zhang, N.; An, Z.; Tsuchikama, K. Glutamic Acid–Valine–Citrulline Linkers Ensure Stability and Efficacy of Antibody–Drug Conjugates in Mice. *Nat. Commun.* **2018**, *9* (1), 2512. https://doi.org/10.1038/s41467-018-04982-3.

(19) Dubowchik, G. M.; Firestone, R. A.; Padilla, L.; Willner, D.; Hofstead, S. J.; Mosure, K.; Knipe, J. O.; Lasch, S. J.; Trail, P. A. Cathepsin B-Labile Dipeptide Linkers for Lysosomal Release of Doxorubicin from Internalizing Immunoconjugates: Model Studies of Enzymatic Drug Release and Antigen-Specific in Vitro Anticancer Activity. *Bioconjug. Chem.* **2002**, *13* (4), 855–869. https://doi.org/10.1021/bc025536j.

(20) Poreba, M.; Groborz, K.; Vizovisek, M.; Maruggi, M.; Turk, D.; Turk, B.; Powis, G.; Drag, M.; Salvesen, G. S. Fluorescent Probes towards Selective Cathepsin B Detection and Visualization in Cancer Cells and Patient Samples. *Chem. Sci.* **2019**, *10* (36), 8461–8477. https://doi.org/10.1039/C9SC00997C.

(21) Vidmar, R.; Vizovišek, M.; Turk, D.; Turk, B.; Fonović, M. Protease Cleavage Site Fingerprinting by Label-Free in-Gel Degradomics Reveals PH-Dependent Specificity Switch of Legumain. *EMBO J.* **2017**, *36* (16), 2455–2465. https://doi.org/10.15252/embj.201796750.

(22) McCombs, J. R.; Owen, S. C. Antibody Drug Conjugates: Design and Selection of Linker, Payload and Conjugation Chemistry. *AAPS J.* **2015**, *17* (2), 339–351. https://doi.org/10.1208/s12248-014-9710-8.